3DS
Digital Die Design System

Final Report

December 2005

Contributors: The 3DS Consortium

Editor: Naomichi Mori / CIMTOPS CORPORATION

1. Summary of Project

1.1 Introduction

The 3DS project was carried out as part of the Intelligent Manufacturing Systems (IMS) program, by an international consortium comprising partners from Japan, the EU, Canada and Switzerland. The 3DS project started in 1995 and successfully finished its phase I in 2003 and its phase II in 2005.

The ultimate goal of 3DS project was to develop a digital die design system (3DS) for sheet metal forming process. 3DS would be a software capable of aiding the designing of a sheet-metal stamping die and its try-out on a computer, eliminating thus the costly and time-consuming try-out on site as currently practiced.

In this project, the following three main subjects were studied intensively.
The main subject was to construct a set of standard benchmark test problems which enabled us to evaluate the ability of a code to predict forming defects such as wrinkle, geometrical inaccuracy due to springback, surface deflection and so on. In the benchmark problems, reference experimental data played a very important role and international cooperation is indispensable to obtain well-examined worldwide standard experimental data.

The second subject was to develop the definition and the quantitative evaluation method of geometrical forming defects. Graphical software library was also developed to construct a forming defect evaluation processor system for illustrating defined forming defects quantitatively on the computer. This processor system provided an important tool for comparing experimental and simulation results of the benchmark problems.

The third subject was to develop guidelines for constructing appropriate elasto-plastic constitutive models for different steel and aluminum sheets, and realistic friction models. The standard material and friction tests were developed to find out the parameters used in the computer simulation.

The standard technologies developed in the research formed the basis for realizing the ultimate objective of the 3DS project of constructing an intelligent sheet metal forming die design system.

1.2 Project Objectives

Stamping of sheet metal is a very important and general process not only used for the production of car bodies, its principal application, but also in the appliance industry, etc. The

process consists in plastically forming of a sheet metal by means of a special set of tools individually made for each part and mounted on a stamping press. The design and fabrication of these tools are an important economic concern. As long as mild steels are used for this fabrication and because, as these are a ductile material, the shape of the part was well related to the shape that of the tool itself. The tool design is then simplified. There was an important progress in the area of machining over the last fifteen years, and this was the advent of CNC machines capable of being operated with data in electronic format, replacing the manually controlled milling machines. In the manufacturing of pressing tools, the new technology was fully exploited by directly using the geometric part definition, the so-called CAD for the machining avoiding the former time-consuming work of manually drawing a tool from the part definition. Parallel to this progress, the fast development of computer simulation started in the ninety's, particularly with the help of the so-called Finite Element Method, allowed developing dedicated software able to help the design of tools by predicting the forming behavior of the sheet metal during stamping.

Today, the codes based upon this technique are really efficient to predict thickness variations, fracture or wrinkling of the sheet in the tool. However, there is still a phenomenon which is insufficiently well predicted: this is the springback. This project was entirely devoted to improvement of the simulation of this defect. Let us first see what exactly the springback is.
When a sheet metal component, after being formed in a die, is removed from the die, also when the scrap area around the contour of the component is removed, springback may occur. In other words, the component loses its desired shape: it no longer conforms to the tool. One major reason for this springback is the presence of residual stresses in the component. The differences between the stresses acting on the inner side and those on the outer side of the component can be decisive for the amount of springback.
When using "new" materials; High and very High Tensile Strength steels and aluminum alloys, highest springback appears. Correct predictions of the amount of springback are difficult even for very experienced and competent engineers. After having been built, the tools need be tested thoroughly and modified to compensate for the springback. These tests, following the "test and error" tactic, are both expensive and time consuming.
Instead of performing these costly tests, it would be very advantageous to be able to predict more precise the behavior of a certain material through simulation of a specific forming process. Spring-back is a very complicated phenomenon, and so numerous simplifications are necessary to represent it with the FEM codes available today, and generate a formula that is fast and convergent.
Due to the importance of the challenge, many studies have been conducted in the world to improve this situation. In our project, four goals were set:

- to define reliable benchmarks that can be used to check the validity of springback

prediction by dedicated software,

- to elaborate a thoroughly established data bank containing information on the materials the most widely used for car body parts to be used in the benchmarks
- to improve the performances of the codes developed by the partners, in terms of accuracy and fastness,
- to develop software able to automatically compare the geometrical definition of parts (CAD), the results of calculations (CAE) and the measurements of stamped parts (CMM).

1.3 Project Structure

The project partners have backgrounds in the product and process engineering and/or in the computer and engineering sciences. All the partners have specific know-how in the area of sheet metal forming processes. Their participation was strongly required in view of the large amount of experimental work (benchmark tests, identification of material and friction laws) and of the numerical simulations which are necessary to achieve highly reliable data.

2. Work Packages

2.1 Work Package Plan

The following three work packages were proposed and implemented.

WP1: Development of user-friendly methods and software for evaluating forming defects.

WP2: Evaluation and improvement of the ability of numerical software to predict forming defects.

WP3: Selection of appropriate physical models and their identification.

All of the three work packages are very closely related with each other as shown in Figure 1.

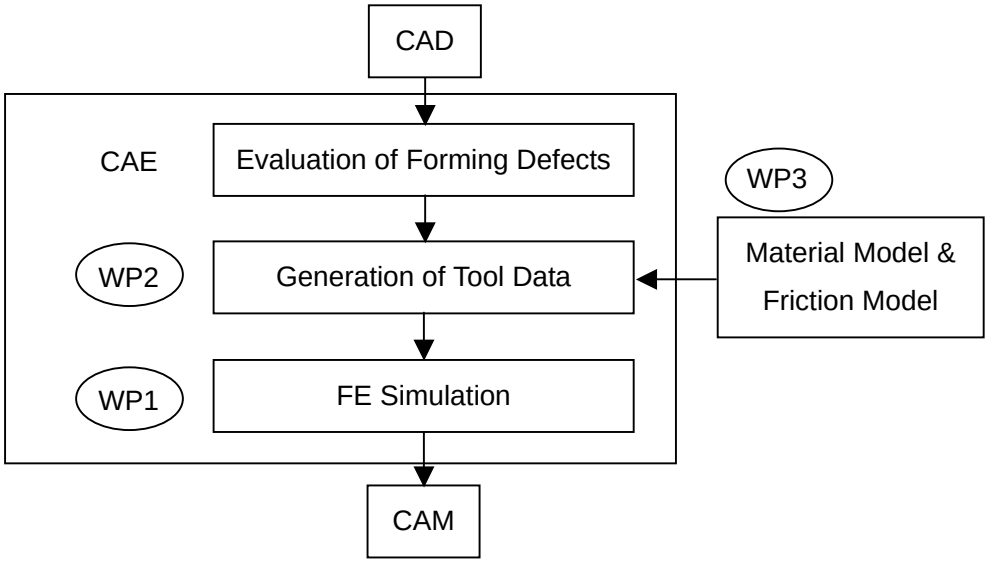

Figure1. Relation among Work Packages

Workpackage 1: Development of user-friendly methods and software for evaluating forming defects

Scope and objectives:

The existence of forming defects is currently checked by means of visual, tactile or mechanical inspection, a process that can hardly be systematized, due to the difficulty of comparing actual products and designed products on a quantitative basis. Another problem concerns the use of numerical results obtained through simulation to evaluate the formability and to make comparisons with designed products. For example, when evaluating the amount of "springback" of a part that has a complicated three-dimensional shape, it is very difficult to make a meaningful comparison between the resulting numerical shape and the originally designed shape without a sound methodology.

It is thus clear that the prediction and the quantitative evaluation of forming defects requires a unified treatment of three different types of geometrical data: CAD data as reference models, which are represented as surface models, CAE data resulting from computer simulations, which are represented as nodal co-ordinates of the mesh and measurement data from real physical objects, which are represented as co-ordinates of some selected points. The goal of WP1 is to establish a methodology for characterizing and evaluating the forming defects. The methodology should be incorporated into a user-friendly, digital environment, and a numerical tool which can be utilized even without possessing outstanding skills of sheet metal forming processing.

To attain this goal, conventional evaluation methods need to be restructured into a new formula to meet the following three requirements: readable with computer with a high repeatability in representation, simple to implement, and easy to validate.

Description of the work

Task 1: Standardization of object data and necessary conditions for data acquisition

Conventionally, the shapes of real formed products have been examined by visual inspection and measurement, by using such tools as jigs, gauges, calipers, and so on. To make a quantitative evaluation of forming defects and a meaningful comparison, it is essential to treat three different types of geometry integrally. In this task, we aimed at determining common formats for geometrical data such as CAD data, CAE results, and measurements data, and to develop a matching method for co-ordinate systems of different types of data within this task. However, for the common format mentioned above, the data acquisition method should be made under standard conditions. These should consist of measurement procedures and of a method for post-processing the measurement data.

Task 2: Definition of forming defects

It is essential to share clear and compatible definitions of forming defects between different companies and institutes belonging to the consortium. A classification of forming defects and definition of intrinsic values for surface and geometrical defects were developed. Self-sufficient definitions of these features without redundancy were given by using certain extensions of the differential geometry of surfaces. The surface of each defect model has some global features, which describe overall distortions, such as the surface being "bent" or "twisted", and local features, which describe local distortions and their locations.

Task 3: Characterization and evaluation of forming defects

Establishment of a reliable method for characterization and evaluation of forming defects is one of the most important tasks of work package 1. A robust method for the extraction of intrinsic values defined in task 2 from discrete point data such as measurement data or simulation results was developed. A verification method, as well as algorithms for derivation of defect models from examples of the format defined in task 1, were also proposed and tested. Task 3 includes also the developing of a new filtering method for noisy measurement data.

Task 4: Development of a defect evaluation processor

Software modules are needed to systematize the evaluation method of forming defects, because they should replace complicated operations that are usually performed by experienced engineers. The modules consist of functions for calculating the characterization parameters and to recognize the forming defects according to the definitions proposed in task 2. Task 4 provides the basic modules for constructing a forming defect evaluation processor. This software library also includes the graphic modules which can display the location of the forming defects, thus allowing to estimate and control the product quality in the forming process.

Workpackage 2: Evaluation and improvement of the ability of numerical software to predict forming defects

Scope and objectives:

WP2 aims at evaluating and improving the ability of numerical codes to predict such forming defects. An essential task of this Workpackage is to establish, perform and thoroughly document a set of reliable experimental benchmark tests for evaluating the ability of a numerical code to predict forming defects.

We also investigate the characteristics of the numerical methods and codes developed and/or used by the consortium partners, by using the results of the benchmark tests, in order to

develop the most appropriate numerical methods for evaluating forming defects during the product and tool design stage.

Description of the work:

Task 1: Definition of a set of experimental benchmark tests for evaluating numerical methods

In press stamping, a variety of parts, such as a very large and complex-shaped automobile body panel, a thick and large truck frame member, or a medium-sized deeply drawn cup, are formed by using tools that have different sizes, shapes and structures. On the other hand, in the press stamping process, many different forming defects are observed, such as tearing, wrinkling, surface deflection, springback, twisting, and surface damage. It is well known that no single numerical software can simulate all stamping processes and/or predict all types of forming defects. Therefore, appropriate standard benchmark tests are needed, in order to evaluate the applicability of numerical software to a specific process for predicting defects with sufficient accuracy. The aim of this task is to perfectly define the conditions of such tests. To this end eight representative benchmark tests have been selected in order to study a large variety of forming defects (see Figure 2). The first five of these benchmarks make use of different types of rails, which are expected to present respectively 2D-springback (change in shape along the cross section), 3D-springback (change in shape along the cross direction and curvature along the longitudinal direction), warping (curvature along the longitudinal direction), and twisting (twist angle along the longitudinal direction), and a combination of these effects. The sixth test is a panel with a central depressed part, which will present a surface deflection near the indent and a large shape deviation from the CAD geometry before and after trimming, as well as wrinkles on the panel surface. The last two tests consider axisymmetric deep drawing processes leading to wrinkling, earring, or rupture (limiting drawing ratio). On each defined type of tool, 15 different forming conditions were considered, by choosing three different blank holder pressures and five different materials (a mild steel, a high-strength steel, a dual phase steel and two aluminum alloys), as shown in Table 1.

Table 1. Materials to be characterized and used for the benchmarks

Material	Grade	Thickness	Provided by
Al alloy 5xxx	5182-O	1 mm	Pechiney
Al alloy 6xxx	6016-T4	1 mm	Pechiney
Mild steel	DC06	0.7 mm	ARCELOR
HSLA	QSLE340	0.7 mm	Cockerill-Sambre
Dual phase steel	DP600	0.7 mm	ARCELOR

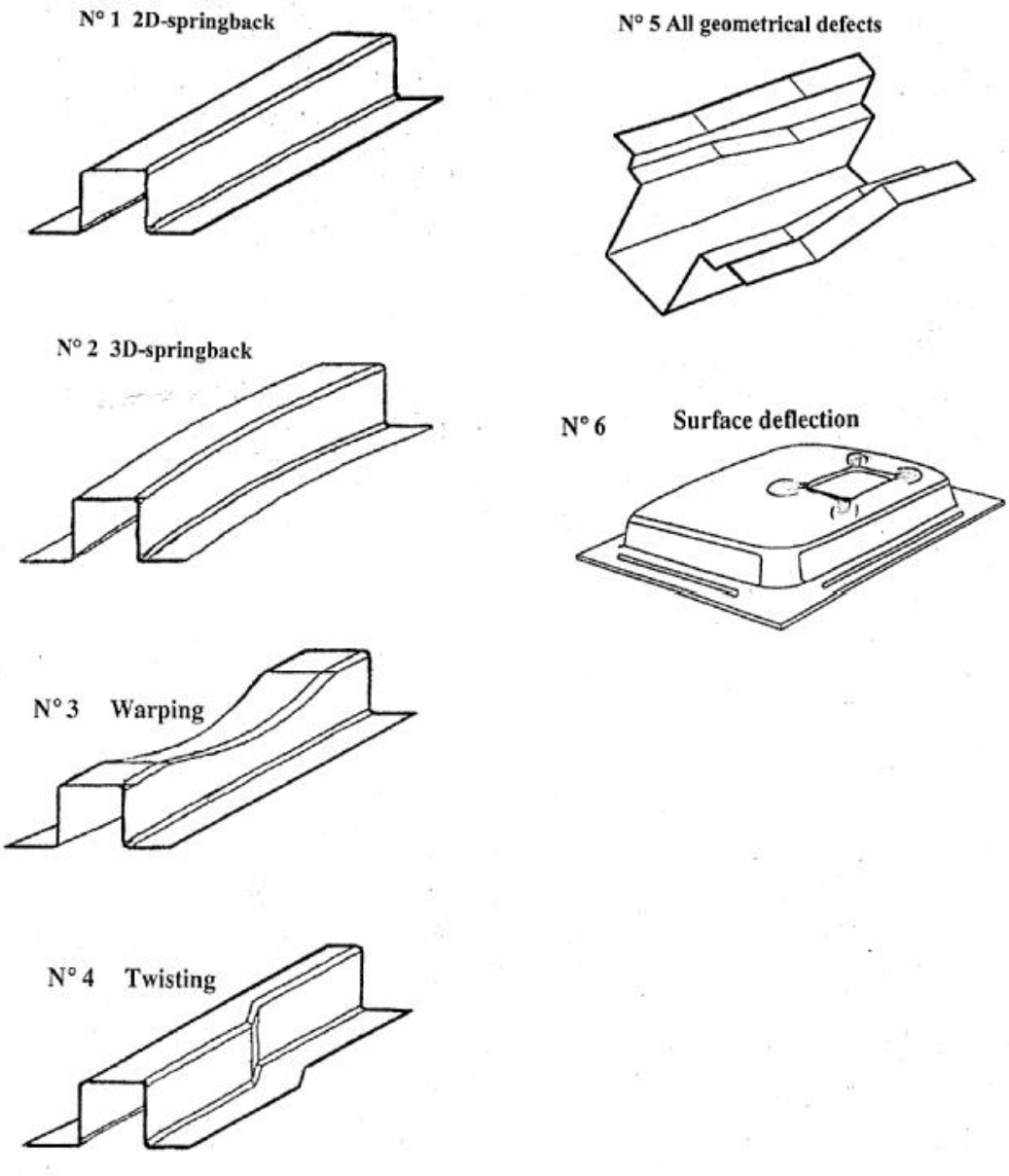

Figure 2. Representation of the eight experimental benchmark tests

Task 2: Carrying out the experimental benchmark tests and geometrical measurement of the parts

The set of benchmark tests defined in task 1 were carried out, thus providing a comprehensive database for the further evaluation of the software ability to predict forming defects. In order to ensure a high reliability of the results, several partners carried out each benchmark. To avoid differences in tooling design and wear, all partners used new stamping tools, of identical design, and produced by the same toolmaker. Furthermore, each contributing partner performed five identical tests for each benchmark, in order to evaluate the

consistency of the results.

The pressed parts were thoroughly measured by each company performing the test, according to the available facilities. For each part produced, experimental data e.g. the evolution of the forming load vs. punch displacement, the thickness distribution along identified cross sections, and the geometrical description of the part shape and defects were collected as reference data for comparison with the results of numerical simulations. The measurements were obtained from devices placed within the stamping tooling, the instrumentation of the press, and from conventional metrology equipment, such as 3D co-ordinate measuring machines. Any case of discrepancy was thoroughly analyzed and the incriminated tests were repeated with the participation of other partners. This represents, of course, a considerable experimental effort, since each test performed by a partner is necessitate the drawing and measurement of at least 75 press parts.

Task 3: Standardization of input-output data for benchmark tests

The input – output data utilized for simulating the forming processes and for evaluating the numerical results should be standardized. In particular, the content of the input data, including the forming condition and the tool geometry must be unified in order to prevent some errors that occur frequently in the evaluation of the numerical methods. This task is closely related to the data formats discussed in WP1.

Task 4: Evaluation and improvement of the ability of numerical methods to predict forming defects

The consortium members numerically simulated the benchmark tests proposed in task 1 by using the finite element codes. It is worth noting that these codes cover almost all numerical strategies currently employed in the simulation of sheet metal forming (dynamic explicit, static explicit, semi- or fully implicit, one-step methods, etc.). On the other hand, the set of codes used by the consortium members include extensively used commercial codes like OPTRIS, AUTOFORM, PAM-STAMP and LS-DYNA, as well as a few codes developed by academic or research institutions belonging to the inter-regional consortium.

This provides an excellent background for a comprehensive and unbiased evaluation of the ability of various types of numerical modeling to predict forming defects and for improving the available numerical strategies. Each consortium partner develops the necessary interfaces that are necessary for implementing the models of elastoplastic and friction behavior selected in WP3 and identified for the five materials. Furthermore, it was intended to perform - for a limited number of the benchmark tests – sensitivity studies concerning the influence of the material and friction parameters and of the finite element mesh on the numerical results obtained.

Workpackage 3: Selection of appropriate physical models and their identification

Scope and objectives

A variety of new sheet materials, such as high strength steels, aluminum alloys, titanium alloys, copper alloys, laminated sheets and coated steel sheets, are on the market. New sheet materials always cause technological difficulties in forming processes mainly because their mechanical and tribological properties during sheet forming are unknown. 3DS could be a powerful tool to overcome these difficulties by using simulations to establish optimum forming methods and forming conditions. However, for the numerical simulation to provide realistic results, accurate and efficient physical models are of primary importance.

Two major physical aspects are involved in sheet metal forming simulation. One is the elastoplastic deformation of sheet metals and the other is the friction between the sheet and tools. Both problems have been addressed by other research projects, too. The originality of our approach is the attempt to obtain the best compromise between the accurate description of the materials behavior and the efficiency of the numerical simulations for steel and aluminum sheets.

Description of the work

Task 1: Selection and identification of elastoplastic and friction models for the materials and tools used in the benchmarks

The main constitutive models considered in this project is isotropic or anisotropic elasticity, initial plastic orthotropy described by Hill'48 model, isotropic and/or non-linear kinematic hardening, rotation of the orthotropy axes at large deformations. The initial anisotropy was determined by uniaxial traction and simple shear tests on specimens oriented at different angles to the rolling direction. The deformation-induced plastic anisotropy was characterized by first deforming large specimens in traction or simple shear. Subsequently cutting out small specimens at different angles to the preshear direction, and subjecting them to either simple traction or simple shear. The results obtained were validated by using plane strain and bulging experiments.

As far as friction is concerned, three different zones should be considered in the deep drawing of sheets: the zone under the blank-holder, where the contact pressure is moderate and the relative displacements between the sheet and the tools are large; the zone on the die radius, where the contact pressure is high and the relative displacements are large, while the friction phenomena combine with plastic deformation; finally, the zone under the punch, where the pressure is low and the relative displacements are small. Therefore, the friction tests

developed in this task simulates as close as possible the contact conditions on these three zones for the tooling, the materials, and the blank-holding pressures used in the experimental benchmarks.

Task 2: Selection of effective numerical algorithms for implementing the physical models into numerical codes

The numerical methods employed in numerical codes make use of various time-integration schemes. To incorporate the elastoplastic and friction models developed in Task 1 into the numerical methods tested by all consortium partners, robust time integration algorithms was developed, checked on standard numerical benchmarks, and optimized. A special contribution was brought by ESI and Autoform, who developed and optimized the implementation of the material and friction models into the commercial code OPTRIS, respectively AUTOFORM, which are used by several partners. The implementation of the material and friction models into the other codes used for numerical simulation were assured by Volvo for LS-DYNA, DaimlerChrysler for INDEED, Renault for PAM-STAMP, CNRS-LPMTM for DD2IMP, FCTUC for DD3IMP, FTI for FAST Suite, NISSAN for ITAS3D and Osaka Inst. for ITAS-Dynamic; this implementation will be made available for the other partners using the same codes.

Task 3: Verification of the appropriateness of the selected physical models for predicting forming defects

The accuracy of the simulation results and efficiency of computation for the physical models selected in task1 and the numerical algorithms implemented in task 2 were evaluated by using sensitivity tests on the benchmarks defined and carried out within WP2.

3. Description of results

Outline of main results is described according to Work packages as follows.

3.1 Work package 1 (Evaluation Processor)

The goal of this Workpackage was to develop a evaluation method and a dedicated software called “Evaluation Processor”, able to compare CAD, measurements and FEM simulation of parts. In this section, the new representation method of springback is proposed. It is strongly helping evaluations and helping to identify the factors of springback such as blank holder forces, gaps between punches and dies, frictions between tools and materials and so on.

The software developed by the Japanese partner has several functions. First it has to correctly fit position data which are not, initially, corresponding. This is made using least square method. As an example, Figure 3 shows the CAD data (red) and measurement point data (white) consisting of 900 and 2522 points respectively. The non-constrained position

fitting result is shown in Figure 4. The fitted measurement point data is converted to the mesh and displayed in green color.

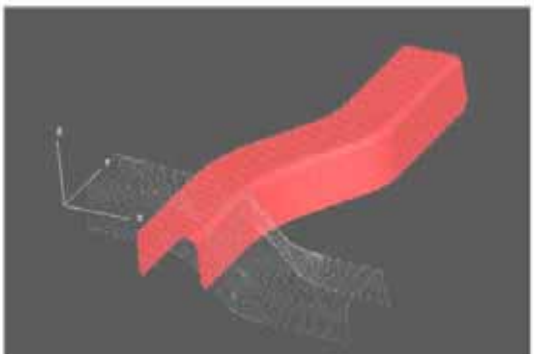

Figure 3. CAD data and Measurement data

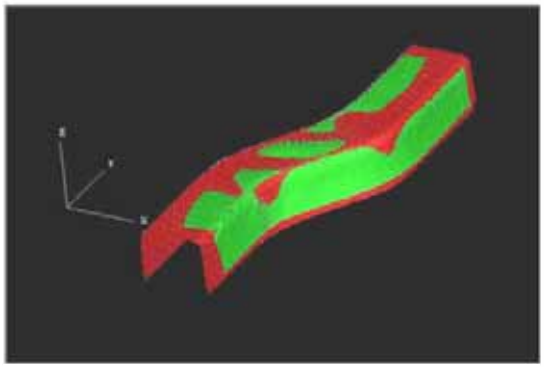

Figure 4. Fitted Measurement data

Second, it allows comparison. What were the problems existing with previous evaluation methods? Figure 5 shows the benchmark test in NUMISHEET'93 and the results of wall curvature as measured by ten participants. As can be seen, scatter is considerable.

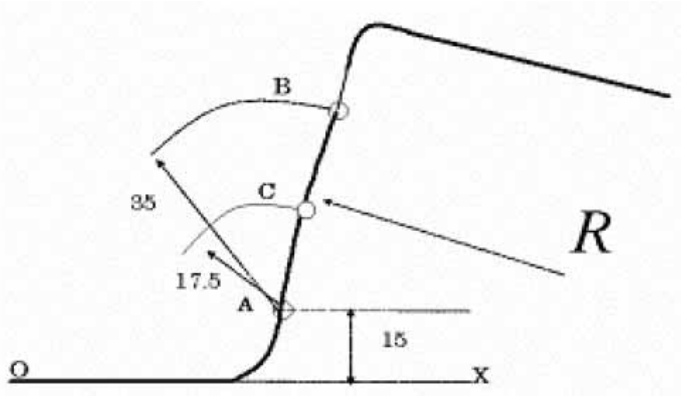

	R
	158.0
	979.3
	118.0
	287.6
	305.8
	335.8
	364.0
	240.5
	375.1
	575.0
AVG.	373.91
Std. Dev.	**247.31**

Figure 5. Previous evaluation method and results of ten participants

The base line **OX** is defined and point **A**, **B** and **C** are measured based on the line **OX** to calculate the radius **R**. Because the **OX** is not flat, the measurement points are changed whenever they are measured even when the same product is measured. Figure 5 also shows ten evaluation results formed and measured by ten participants. Because the big deviation of **R** is occurring, this evaluation method is not appropriate for the standard evaluation. The reason why the big deviation occurs is that **R** changes too sensitively on the positions of **A**, **B** and **C**.

Taking into account the previous problems, a new representation method of springback for computerized evaluation was developed. The continuous curvature is used to characterize the defects, because, especially on the sidewall, big deviation will happen if we use only one curvature value. The continuous angle is also used to characterize the defects.

To satisfy these, we need a certain extent number of measurement points. Our proposed method utilizes the points measured by CMM (Coordinate Measurement Machine). Figure 6 shows the measurement of the product using fixtures, since Figure 7 shows the measured points. In this example, the measurement pitch (the distance of two points) is 2.5mm. Following is an example of usage of curvature profile: the side wall curvature.

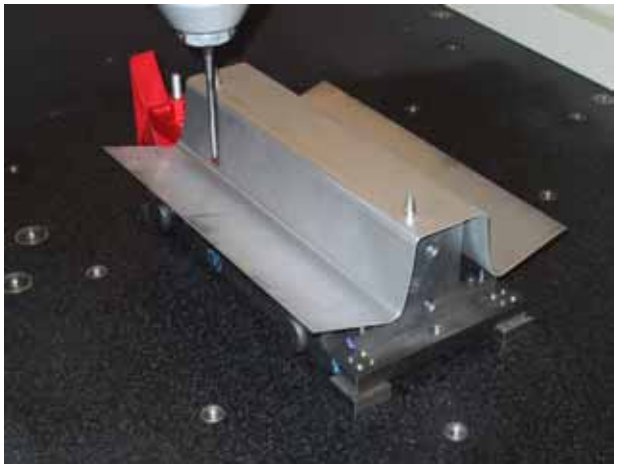

Figure 6. Measuring system

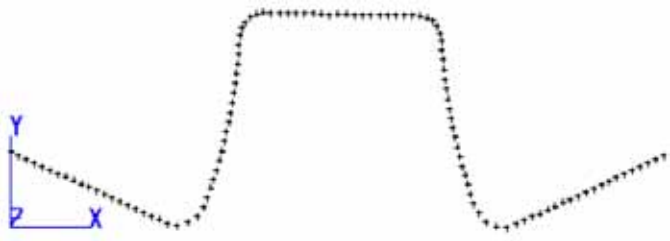

Figure 7. Measurement points data

In the curvature profile, **BC** and **FG** are nearly straight, so two side wall curvatures may be approximated by averaging curvatures between **BC** and **FG**. The approximated sidewall curvatures are shown in Figure 8 after treatment.

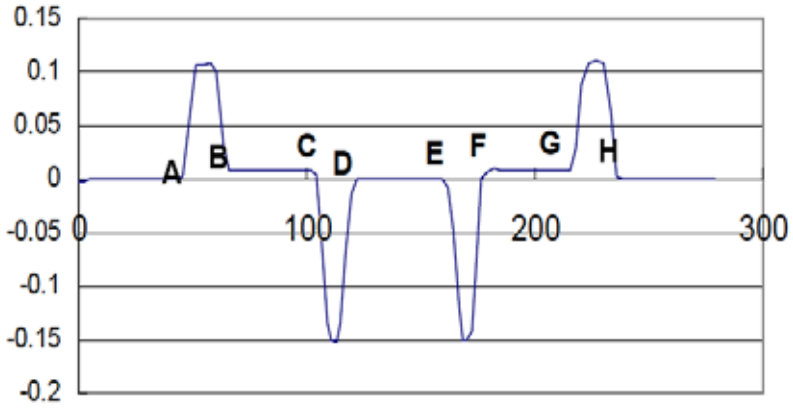

Figure 8. Curvature variation along the curvilinear abscissa

Another possibility of representation of the profile variations is to consider the angles variation along the profile. This mode has proved to be very efficient and was the most widely used by partners during the project. An example of the profile shown in preceding figures is visible on figure 9.

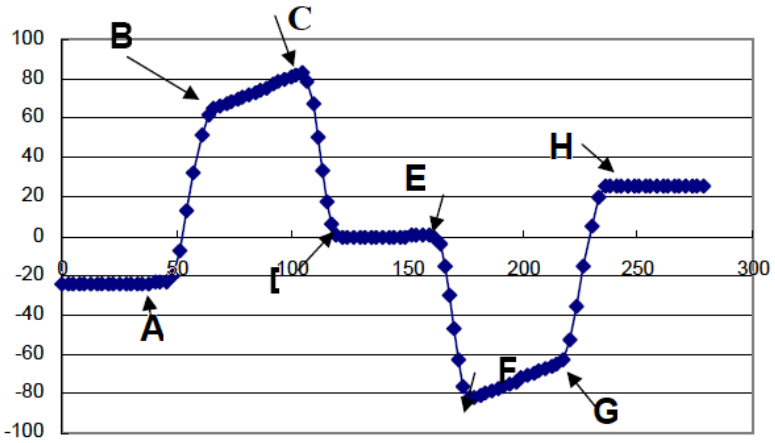

Figure 9. Curvature variation along the curvilinear abscissa

This technique revealed itself as being less noisy and easier to interpret. Very subtle modifications of shape can be analyzed with reference to the parameters of forming. For example, it allowed us to identify the case where there was a sliding of the blank on the punch nose. The flatness of the material on punch nose is also easily identified and it corresponds to the straightness of the segment DE. Curvature of the wall is visible on segments BC and EG: the more slope they exhibit, the highest is the curvature.

In conclusion, the software developed in the Workpackage 1 completely fulfilled the demand for an easy comparison of data coming from calculations and experiments.

3.2 Work package 2 (Benchmarks)

The important task of the project, the basis for all the rest of the program, was to perform benchmarks in order to judge the reproducibility of stamping process when carried out in different places but following the same procedure. The goal was to determine how these experiments are reliable databases for simulation calculations evaluation.

During the 3DS project duration, more than 800 experimental parts were realized on hydraulic presses in laboratories or press shops. This chapter reports on principal results obtained. We rapidly present the tools that were used in the project: five rails and a panel. Each tool was designed in order that the parts made with exhibit a special type of springback defect. Figure 10 shows the rail of benchmark #1. It is the classical straight part which exhibit very much springback due to its lack of transverse stiffness.

Figure 10. Rail #1

On figure 11 is the rail #2, a bowed part designed to present a 3D deformation.

Figure 11. Part obtained with tool #2

Part #3 was done in such a way that wrinkling appeared at the start of forming. The goal was to assess the way this wrinkling was modifying the springback and to check if it was taken into account by numerical simulation.

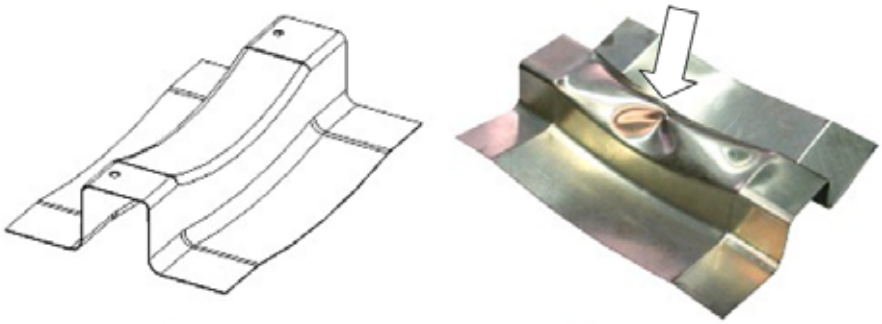

Figure 12. Wrinkling (arrow) on a part of type #3

Tool #4 was a more complicated one. The main idea was that the variable cross section would crate a tendency to twisting.

Figure 13. Varying section of part of type #4

With tool #5, imagined by the partner DaimlerChrysler, the very complex shape was designed in order to produce several bending-unbending successive operations during forming, thus giving importance to the kinematic hardening tendency of the material.

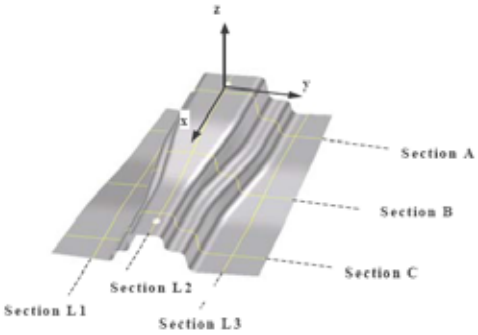

Figure 14. Complex shape of tool #5

Finally, the panel #6 was designed with a depression in the central area which is prone to give elastic deflections of the metal around it.

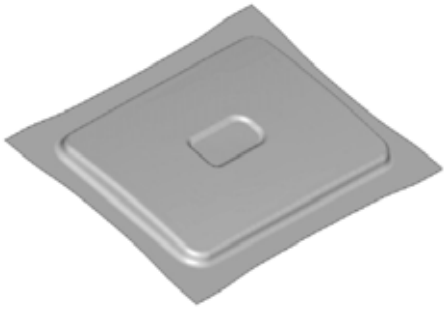

Figure 15. Panel made with tool #6

In certain cases, particularly for aluminum alloys, we observed a strong apparent scatter of results. As long as this scatter was not explained, it was impossible to choose the basis of comparison for the FEM simulations, an important goal of the project. The search for this explanation was very long and difficult and was finally successful. We distinguish two types of scatter when considering the results of tools #1 to #4: “Intra” scatter and “Extra” scatter, the “intra scatter” within results of one participant, and the “extra scatter” between participants.

Although many precautions have been taken, the results showed not a common trend concerning repeatability. Many experiments gave the same results in terms of punch force and profile, but some of them gave systematic variations between partners while others were even giving variations for a single partner. An example of results showing good repeatability is shown in figure 16. This is rail #4 and dual phase steel. Both geometry and material characteristics are responsible for such good repeatability in results. The chosen defined experimental variables were perfectly adjusted for this situation.

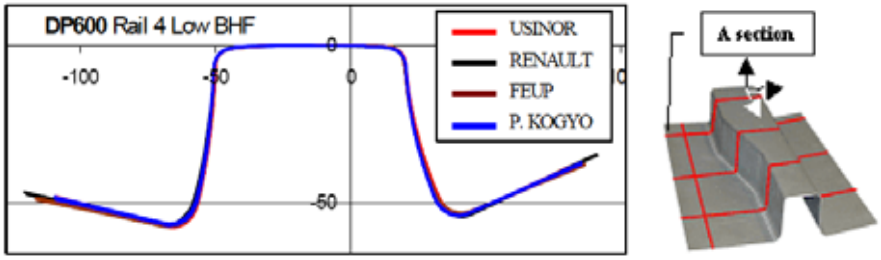

Figure 16 Repeatability of results for several different partners – rail #4, DP600 steel

However for some other geometry/material couplings, the same experimental conditions were not completely adjusted for obtaining such a good repeatability of results. This section analyses observed variations within a single partner, while next section analyses variations between partners. In figure 17 is shown the variation observed for rail #1 for a single partner (particularly on left side). By measuring the final flange lengths of the rail parts it was demonstrated that during stamping the blank slides over the punch.

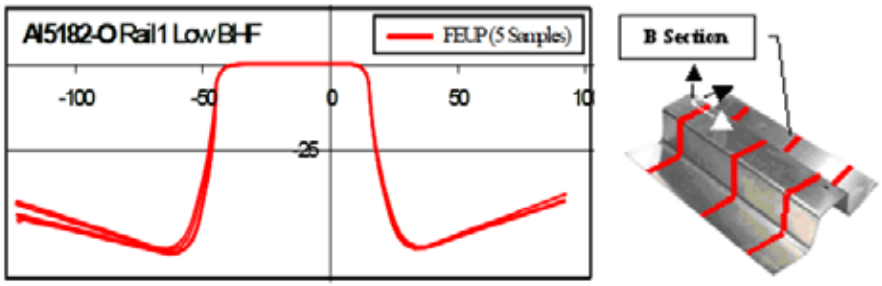

Figure 17. Variation of results for a single partner – rail #1, aluminium AA5182

Later experiments with the same material and same experimental conditions, but with blank movement restriction over the punch showed a perfect repeatability. In figure 18 we may see experiments with and without restriction: the no restriction case (red) gives variation for final geometries while the case with movement restriction leads to very reproducible profiles.

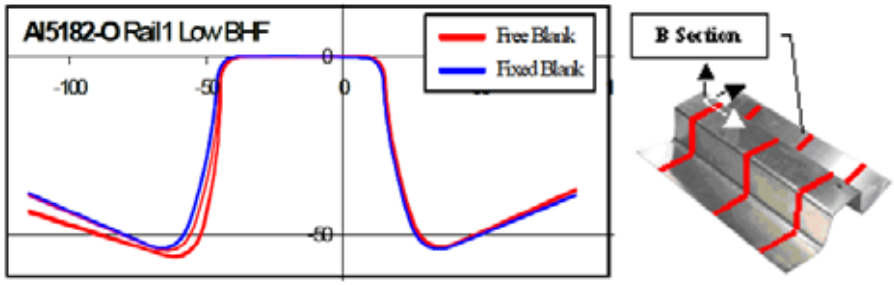

Figure 18. Influence of fixing blank for AA5182 – measured profiles

To eliminate the influence of this “internal” scatter, flanges of all parts were measured and those showing anomalies were eliminated from the final statistics. Such a selection is of course easy in case of tool #1 or #3 where flanges should be symmetric, but more complicated in case of tools #2 or #4. The following table 2 gives an example of the selection policy used. It concerns tool #2 and an aluminum alloy. It can be seen that with the 200 kN blank holder force, the flanges are about 65 mm on one side and 53 mm on the other. When passing to the 300 kN blank holder force, it is normal that both flanges increased since the friction restraining force increases itself. So the values 66 mm and 55.8 mm are very logical. However, four of the five samples have very much slid on the punch, leaving flanges of 5 mm more on the hole side and 5 mm less on the opposite side. They were eliminated. It can be observed that a simple statistical treatment (for example the Student test) would not be convenient in such a case: the only good result would be eliminated. It was, in this case, necessary to use physics and logic to solve the problem.

Table 2. Mode of elimination of abnormal flange lengths

Blank holder force	Code	Hole side	Opposite side	
200	E0152M1	63.5	54	no slid
200	E0152M2	64	53.7	no slid
200	E0152M3	65.5	52.5	no slid
200	E0152M4	64.5	53	no slid
200	E0152M5	64	53.5	no slid
300	E0152H1	71	50.5	slid
300	E0152H2	66	55.8	no slid
300	E0152H3	71.5	50	slid
300	E0152H4	70	50.5	slid
300	E0152H5	70.7	50	slid

The reasons behind the variation of results seen in previous section could not explain the occurrence of variations between different partners as shown in figure 19 for rail #1, after taking out the “Intra” variation.

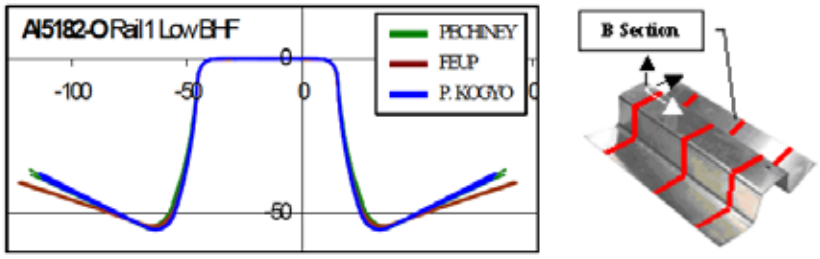

Figure 19. Results from several partners of measured profiles for rail #1 and AA5182.

Clearly, profiles measured by Press Kogyo and Pechiney are identical but different from those measured by FEUP. On figure 20 is shown an example of recorded forces during forming.

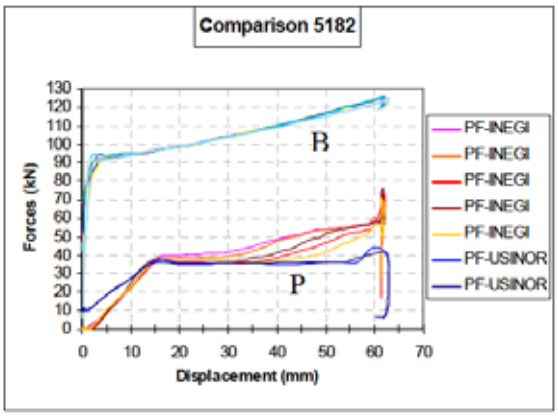

Figure 20. Results from two partners of force/stroke for rail #1 and AA5182

The blank holder force is correct for the two partners, close to 90 kN at the start of forming. This force increases because the gas in gas springs is compressed. Normally, the forces measured at the punch (corresponding to the sum of forming effort and friction forces) should be the same for both partners. However, they are very different in their evolution. It is clear that the increase is not normal as shown now.

During forming of a hot shaped part under constant blank holder force, there is no reason for an evolution of force because there is no shrink drawing or stretching, only a constant bending unbending on the die radius. This was already observed in many experiments.

So, in our case, it would be normal to have a small increase (about 30 %) of the punch force because there is one of the blank holder forces. However, the very large increase observed with FEUP experiments, starting between 30 and 45 mm, is not at all to be considered as normal. It denotes an evolution of some process parameter. Because the blank holder force is under control, because such an evolution of forming effort cannot be due to a sudden variation of material characteristics, a variation of friction must be suspected.

We discovered by comparing data that there was a strong relationship between the maximal punch force attained before the end of forming and the level of springback. It was then possible to look at more classical influences and to prove that ram speed was playing an important role for such variation of results. The graph of figure 21 shows the evolution of the punch forces measured in many experiments.

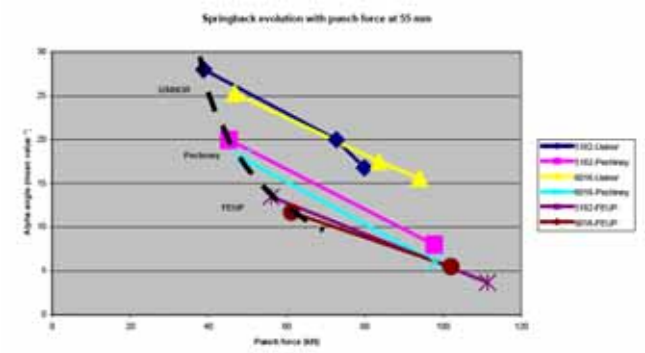

Figure 21. Springback evolution with punch force at 55 mm stroke - Rail #1 and A5182

Two facts are evidenced by this graph. First, for one material and one partner, there is a clear relation between measured punch force at the end of the stroke (X axis) and the mean value of the measured α angle of the flange (Y axis) of the corresponding parts. This result is known since a long time, the principle is even used to reduce springback by a tension applied at the end of forming. So we had the proof that the results were consistent within one partner.

Second, the dotted line also shows that there is an objective reason for the difference of results between partners: for the same material and blank holder force, the α angle deceases when the punch force increases.

This observation leads to the conclusion that the differences observed within partners results (Particularly with aluminum alloys) are not the erratic consequence of hazard - true scatter - but real variations due to real differences in the forming behavior.

We will now schematically present the results part by part.

Tool #1

In some respect, rail #1 is, as already pointed out, one of the most important because it is relatively simple and strongly sensitive to springback.

Four partners were involved in this benchmark:

- FEUP
- Press Kogyo
- Pechiney
- Usinor

All the experimental punch forces have been measured at 20 and 55 mm of stroke to compare the trials. We have seen that the simple comparison of the final forces (around 55

mm of stroke) was very informative. Typical experimental punch forces vs. punch strokes for five identical parts #1 are illustrated in the figure 22 hereafter.

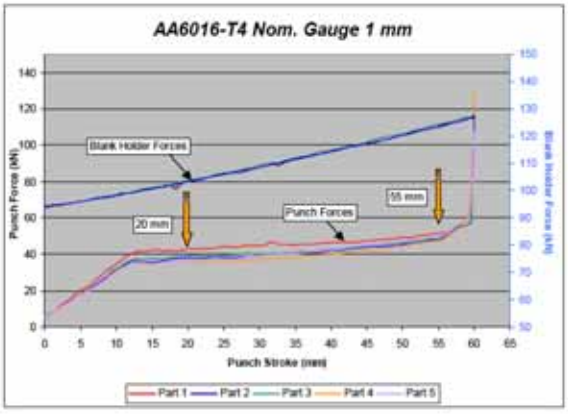

Figure 22 Typical scatter of punch force on tool #1

The synthesis of mean values of measured punch forces is presented in the following table 3.

Table 3: Benchmark #1 – Punch forces measured at 20 and 55 mm

Material	BHF (kN)	Punch force at 20 mm			Punch force at 55 mm		
		Pechiney	FEUP	Usinor	Pechiney	FEUP	Usinor
AA5182	90	30.1	35.5	28.1	45.2	56.0	38.8
	200	46.9	46.8	47.8	97.7	111.4	72.7
	300		64.2	58.0		133.6	79.9
AA6016	90	39.8	42.2	39.6	48.6	61.2	46.7
	200	85.4	62.8	73.8	98.1	102.0	83.6
	300		84.1	86.9		127.6	94.0
DCO6	90	50.9	47.2	46.1	58.5	53.7	50.0
	200	93.9	83.5	110.4	106.1	105.3	101.2
	300		110.9	115.5		139.4	120.7
HSLA	90	62.7	57.0	59.8	74.4	71.6	63.7
	200	112.8	109.5	110.4	129.4	131.8	116.4
	300		164.6	153.8		164.6	153.8
DP600	90	54.7	52.6	51.7	61.6	66.3	56.4
	200	94.6	88.8	96.5	110.6	114.4	105.5
	300		130.0	130.9		154.3	146.7

Although the forces measured at 20 mm stroke are well correlated, we see that in certain aluminum tests the force at 55 mm can be as high as 2.4 times the 20 mm force (FEUP, AA5182–Medium BHF). Such an increase is indeed completely abnormal. Comparatively, Pechiney or Usinor recorded increases contained between 33 to 50 %. Results for steels were normal. The apparent reason of this undue increase was a ram speed inferior to the wanted value of 20–30 mm/s. FEUP discovered later that the real speed was close to about 10 mm/s. Nevertheless, as already signaled, this difference is not sufficient to explain all results. All parts measurements were made with a 3D measuring machine. All partners used the NXT Post Processor developed by M&M Research to compare the geometrical results obtained. We use the α angle parameter (angle between flange and horizontal) to judge the global result.

Table 4. Comparison of α angles between Pechiney, FEUP and Usinor (mean values)

Material	BHF	Alpha left				Alpha right			
		Pechiney	FEUP	P. Kogyo	Usinor	Pechiney	FEUP	P. Kogyo	Usinor
AA5182	90	20.5	14.7	20.9	27.9	19.6	12.4	20.2	28.3
	200	7.4	4.5		19.0	8.7	4.0		20.9
	300				16.9				15.7
AA6016	90	18.5	12.7	17.8	25.5	17.4	10.6	15.7	26.1
	200	6.3	5.5		17	5.8	5.6		17.9
	300				16.2				17.0
DCO6	90	9.8	6.6		11	8.4	6.7		10.2
	200	4.9	5.0		8.9	4.3	4.7		8.6
	300				7.5				7.3
HSLA	90	16.0	13.7		29.2	16.6	15.5		28.5
	200	12.8	10.9		18.2	11.6	11.7		17.6
	300								
DP600	90	23.7	19.8		29.2	24.1	20.1		28.5
	200	17.0	18.9		27.2	18.3	18.4		27.5
	300				26.4				26.1

Comments:

- the flange angles are symmetric, proving the quality of tooling and experiments,
- they always decrease with the blank holder force, a predictable tendency,
- they strongly differ between partners for aluminum alloys, particularly for AA5182, this being related with differences we saw about final punch forces,
- these differences are less pronounced for steels,
- the ranging between partners is the same for all materials (from less springback to more springback):

Finally, we see that this benchmark was strongly influenced by ram speed differences.

We consider that the flattest punch force curves given by Usinor tests at a correct ram speed of 25 mm/s are probably the most representative of a forming without significant galling. Springback measured in tests made by Press Kogyo and Pechiney seems to be a representative value in the case there is an increase of force with some slight galling.

A very important conclusion is that these benchmark results cannot be used directly to compare with simulation using the same initial conditions, particularly ram speed. Some correction must be done to take into account the effects of ram speed and its variation. In fact, the best solution would probably be to compare these data with simulations assuming the same punch force evolution.

Tool #2

For this tool, the experimental benchmarks were made by Pechiney, FEUP, Press Kogyo and Usinor. For sake of simplification, all data given here (table 5) are taken from the medium section of the part (called B) and only reflect the flange angle with horizontal, called α.

Table 5. Comparison of α angles between Pechiney, FEUP and Usinor (mean values)

Material	BHF (kN)	Alpha left			Alpha right		
		Pechiney	FEUP	Usinor	Pechiney	FEUP	Usinor
AA5182	90	9.6	6.9	8.9	10.2	6.2	8.0
	200		6.8	7.2		5.5	7.9
	300		6.3	7.2		3.0	6.8
AA6016	90	9.0	5.9	8.7	9.7	5.5	8.3
	200		7.0	7.0		4.4	7.5
	300			6.9			6.3
DCO6	90	4.3	2.5	4.1	4.2	2.3	3.2
	200		2.9	3.5		2	3.5
	300		3.3	3.5		2.2	3.0
HSLA	90	6.0	3.9	6.1	7.6	5.7	4.8
	200		3.8	5.7		4.5	4.8
	300		3.5	5.2		3.5	4.5
DP600	90		6.6	8.5		8.2	6.8
	200		6.9	7.9		7.2	6.5
	300		6.8	7.4		6.3	6.7

Compared to those of tool #1, α angles are smaller, due to the higher transverse stiffness of the part, and their variation is also reduced. Angles measured by FEUP have a tendency to be smaller, particularly for aluminum alloys, but the agreement between partners is nevertheless acceptable, the difference in angle being rarely more than 2 degrees.

Tool #3

Several partners have performed experiments with tool #3. However, profile measurements of such experiments have been only performed by FEUP, due to the time needed for. Five profiles were measured on each part. To simplify the presentation, we give only the mean values of flange angle α1 and α2 as measured on profile A.

Table 6. Measured α angles

Material	BHF (kN)	Angle α1 (°)		Angle α2 (°)	
		FEUP	Usinor	FEUP	Usinor
AA5182	90	12.6	12.8	12.1	12.9
AA6016	90	11.0	11.7	10.2	12.4
DCO6	90	5.2	4.4	6.0	5.0
	200	1.5	3.9	1.5	3.5
	300	0.6	1.6	1.1	1.6
HSLA	90	11.0	8.7	10.9	8.7
	200	3.6	5.9	3.7	5.9
DP600	90	17.1	14.9	17.5	14.9
	200	11.6	11.9	12.0	12.1
	300	10.7	9.9	11.6	9.6

In general, results are close together. We see again that the flange angle decreases with the blank holder force for a given material, a logical result. When comparing steels between them, it's also clear that the DP600 is more prone to springback than HSLA and, above all, DC06.

Tool #4

Four partners were involved in this benchmark: Usinor, FEUP, Press Kogyo and Renault. Usinor and FEUP did all their trials, Press Kogyo and Renault did only trials at low blank

holder force condition. As accustom, some steel results are with an excellent reproducibility, as shown for example by figure 23 for DP600 steel at lower BHF. Aluminum alloys generate more scatter.

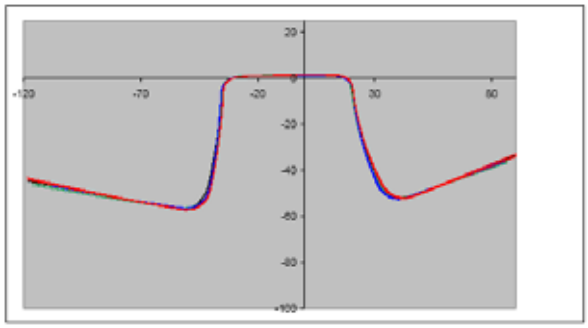

Figure 23. Steel DP600, low blank holder force

Discrepancy for each partner is lower than ±1°. Detailed results are given in table 7. In this particular case are indicated not the α angles but θ 3 and θ 6 angles corresponding to the walls.

Table 7. Measured θ angles, section A

Material	BHF	θ3 angle (°)				θ6 angle (°)			
		Renault	FEUP	Usinor	P. Kogyo	Renault	FEUP	Usinor	P. Kogyo
AA5182	90	9.8	9.9	10.6	12.5	16.8	13.4	15.8	15.9
AA6016	90	8.4	9.4	9.3	10.7	14.7	11.9	14.2	14.5
DCO6	90	3.1	3.7	3.1	3.2	5.7	1.5	1.8	4.6
HSLA	90	5.8	6.0	6.8	7.1	10.9	8.7	8.8	9.9
DP600	90	11.4	10.3	9.5	11.5	18.2	17.3	17.4	18.3

We observe that angles θ 3 are in very good agreement for all materials. The reason is that this side of the part is rigidified in the longitudinal direction compared to the other side which is completely straight.

Maximum differences in θ 6 angles between average results of partners (by materials) are:

- 5182 3.4 ° ,
- 6016 2.8 ° ,
- DC06 4.2 ° ,
- HSLA 2.2 ° ,
- DP600 2.0 ° .

Strange enough, the maximum of difference would be, for this tool #4, with the DC06 steel, particularly if we consider the small value of measured angles. We have no explanation for it. All other results can be considered as very reproducible. We chose to evaluate twisting only in top of rail. Two segments are defined in section A and C. Segments are projected in 0yz plane and the angle of twisting is measured between these two projected segments. Twisting angle evaluation was made only at low blank-holder force. The average angle for DC06 is ~ 0°. All other materials twist in same direction. Along X-axis, twisting is in clockwise direction. This is

shown in Table 8.

Table 8. Measured twisting angles

Material	Min (°)	Max (°)
AA5182	+0.01	+1.11
AA6016	+0.06	+0.66
DC06	-0.43	+0.51
HSLA	-0.27	+0.82
DP600	+0.80	+1.93

In general twisting is not so strong. We would have preferred more for our study.

Tool #5

Due to the tool failure during tests in Volvo plant, we have only one series of results, due to DaimlerChrysler. So no comparison is possible and this analysis will be short.

As for other rails, blank holder forces of 90, 200 and 300 kN have been tested. Because of the asymmetry of the part geometry, the results interpretation is very difficult, especially to characterize numerically the amount of springback. Options chosen for tools #1 through 4 are no longer valid. An idea of how complex is the interpretation of results is given by the graph of figure 24. On one profile, flat areas have been chosen and the deviation (in mm) between measured points and expected points (as defined by the CAD) is plotted. For example, section for X=25 mm (one extremity) is represented by points 1 to 23, section for X=125 mm by points 24 to 45 and so on. Clearly, only a patient and detailed comparison of many graphs of this kind is able to give some understanding of complicated phenomenon. No simple way has been found to schematize them.

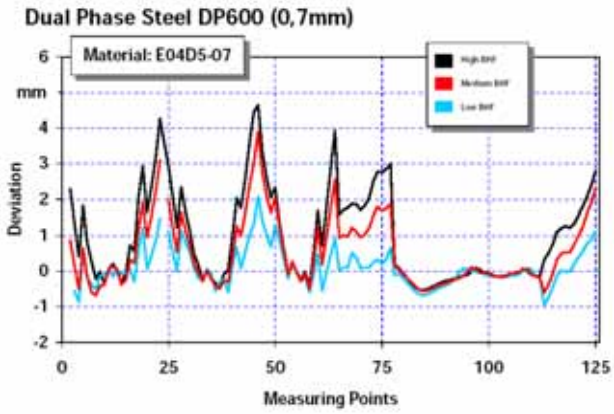

Figure 24. A graph corresponding to one section of a part made with tool #5

One observation can be made. The blank holder influence has a tendency opposite to the classical one: springback increases when blank holder force increases. We think that the explanation comes from the fact that the first part of the stroke only put in tension the material, without any forming (no contact with the steps of the die). Resulting from straining, the metal

would thus be strain-hardened before bending on the steps.

The higher the BHF, the higher would be the strain hardening and thus the springback (because of yield strength increase). This hypothesis is currently under verification. It can be noted that this strange result is of interest because many industrial parts are more or less looking like this tool #5 part.

Tool #6

Several parameters are of interest on this panel.

The draw-in is the quantity by which has the material been moved in the tool. It was measured both as the flange length after forming and as the total length after springback.

Table 9**.** Draw in measurements. The values are average values from the test panels.

Material	Co.	Dx1	Dx2	Dy1	Dy2
DC06	Nissan	41,7	41	45,1	45,1
	Volvo	40,1	39,9	42,6	42
	Renault	44,8	44,1	38,9	39,7
	Cockerill				
HSLA	Nissan	37,5	36,5	42,3	42,1
	Volvo	37	37	41	42
	Renault	35,7	36	38,2	39,8
	Cockerill	30,5	31	37	37
AA6016	Nissan	43,2	42,5	47,1	47,2
	Volvo	42,5	42,5	46	47
	Renault	43	43	43	43,2
	Cockerill				
DP600	Volvo	37,4	36,9	40,6	42,1

The results are the same for Volvo and Nissan. They are slightly different for Renault; one reason could be the appearance of hard points during the trials, which restrict the draw-in and are difficult to control. We can also signal that the influence of small differences in lubricant amount was demonstrated in this study by Volvo.

In the case of HSLA tested by Cockerill, the depth of the parts was too high. The springback behavior was evaluated by analyzing different section after springback. The position of the sections can be seen in figure 25.

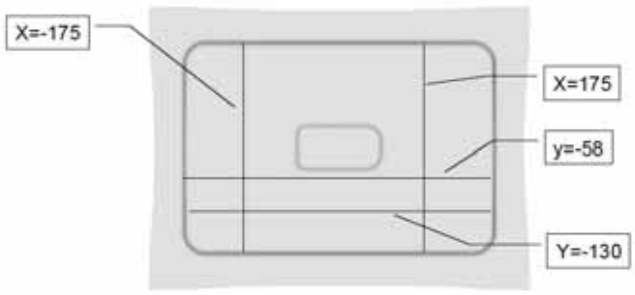

Figure 25. Positions of evaluated sections

All experimental results cannot be displayed here. Below is an example of section y=-58 shown (figure 26). All partners did not report all sections and materials, but for this section are there results available from concerned partners. The results from the different partners are reported in the same color. In Volvo's results is the variation in the experiments marked with a vertical bar (max/min-value)

Note: 2nd and 3rd figures indicate the partner: Cockerill=02, Volvo=04, Renault=05, Nissan=16

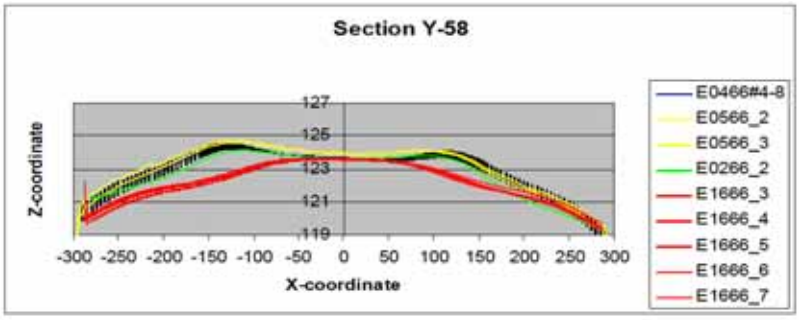

Figure 26. Experimental results for AA6016

The surface quality was evaluated by measuring points over the surface. Different partners used different systems. The points were then imported in the NXT post processor and evaluated with fixed parameters in order to have the same references for all partners. Here is an example of such evaluation.

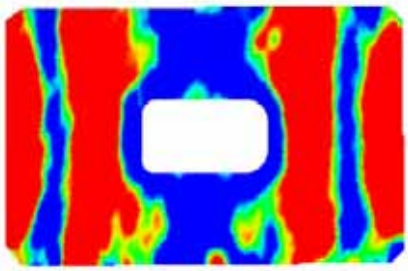

Figure 27. Experimental results DP600 (Volvo Part n°5)

The different partners achieved relatively similar results regarding the qualitative aspect. However the quantitative agreement was less accurate. This indicates that the tool gives relative stable results but the different process set-ups generate differences in results. Furthermore was the appearance of "teddy bear ears" small but visible. Other defects as unstable surface where much more dominant.

As a general conclusion about these benchmarks, we can say that all the programmed ones in the 3DS project have been realized in their large majority. Some exceptions result from the

capacity of the presses used or from unexpected difficulties. However, more than eight hundreds experiments have been carried out. This constitutes a fantastic bank of results, so much that all their exploitation was not possible in the course of this project: there are more that 15000 angles measured, only for rail type parts.

Many of the results show a good reproducibility between the experiments realized by the different partners and can be directly used as reference values. However, we have observed some cases with an apparently large scatter, but a very long and meticulous examination of the parts, the blank holder forces and the punch forces evolution, has opened a way for the comprehension of this scatter.

Ram speed was recognized as a prominent factor of reproducibility. Ram speed must be interpreted in a large sense: not only its mean value has an influence but also its evolution near the end of stroke. This is a very important point which was clearly demonstrated. It makes more difficult the use of experimental results and could explain many discrepancies observed in previous benchmarks performed by other instance, for example in the Numisheet conferences.

3.3 Work package 3 (Software improvement)

The aim of this work was to compare the results of the simulations made with the data coming from the numerous benchmarks executed in the course of our project.

Hundreds of FEM simulations were performed by the partners in order to:

- first simulate the forming of parts (rails and panels),
- secondly predict the amount of springback of these parts.

We used six different codes:

- one software developed by the University of Coimbra, named “DD3IMP”,
- a commercial software developed by Dynamic Software, called “OPTRIS”,
- a commercial software developed by ESI, named “PAMSTAMP”,
- a new version of this software called “PAMSTAMP2G”,
- a commercial software developed by Livermore Software Technology Corporation named “LS-DYNA”,
- a commercial software developed by AutoForm Engineering GmbH, named “AUTOFORM-incremental”.

Various types of physical models can be used for the description of plastic anisotropy at large strains, according to their required ability to explain and/or predict the details of the plastic behavior during a given deformation process.

“Selection of effective numerical algorithms for implementing the physical models into numerical codes”.

The physical models selected and implemented in the FEM codes were the following:

- Isotropic work hardening described by the Swift law,

- Isotropic work hardening described by the Voce law,
- Isotropic work hardening described by the Swift law combined with a kinematic work hardening described by Lemaître and Chaboche law,
- Isotropic work hardening described by a Voce law combined with a kinematic work hardening model described by Lemaître and Chaboche law,
- Complete and simplified micro structural model.

The yield surface is described in all the five models by the orthotropic Hill'48 yield criterion.

Benchmark #1

All partners involved in the tool #1 benchmark have used the NXT Post Processor developed by M&M Research to compare the simulation geometrical results with the ones experimentally obtained.

Two different solutions were used concerning the coefficient of friction:

- a common value of 0.1, which is an usual figure,
- variable values adapted to each part of the tool, as measured experimentally in the WP3, ask1 They are:

Blank/BH = 0.21, blank/die radius = 0.25, blank/punch = 0.3

Available calculations for tool #1 are summarized on the following table.

Table 10. Available calculations for tool #1

Partner	Code	BHF	Hardening law	Friction	5182	6016	DC06	HSLA	DP600
AutoForm	AF-I	90	Swift	0.1	OK	OK	OK	OK	OK
ESI	P-S	90	Swith+kin.	0.1	OK	OK	OK	OK	OK
ESI	P-S	90	Voce+kin.	0.1	OK	OK	OK	OK	OK
Pechiney	Optris	90	Hock-Sher	0.1	OK	OK			
Pechiney	Optris	90	Voce+kin.	0.1	OK	OK			
Pechiney	Optris	90	Hock-Sher	Variable	OK	OK			
Pechiney	Optris	90	Voce+kin.	Variable	OK	OK			
DaimlerChrysler	P-S	90	Swith+kin.	0.1	OK	OK	OK	OK	OK
Usinor	AF-I	90	Swift	0.1	OK	OK	OK	OK	OK
AutoForm	AF-I	200	Swift	0.1	OK	OK	OK	OK	OK
ESI	P-S	200	Swith+kin.	0.1	OK	OK	OK	OK	OK
AutoForm	AF-I	300	Swift	0.1	OK	OK	OK	OK	OK
ESI	P-S	300	Swith+kin.	0.1	OK	OK	OK	OK	OK

It has been shown that experiments were "polluted" by unexpected variations of friction, something probably due to some form of galling. Such a phenomenon cannot be, of course, reproduced in a normal simulation.

Remark: it could be in some special cases, using an evolutive law of friction, but such a solution has no industrial interest since galling must be avoided as much as possible.

For this reason, comparison of forces can only be made at start of forming that is 20 mm stroke. These comparisons are presented in figures 28 to 30.

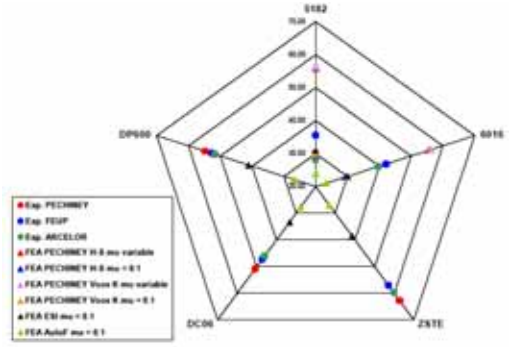

Figure 28. Experimental forces compared to calculated ones – Low BHF

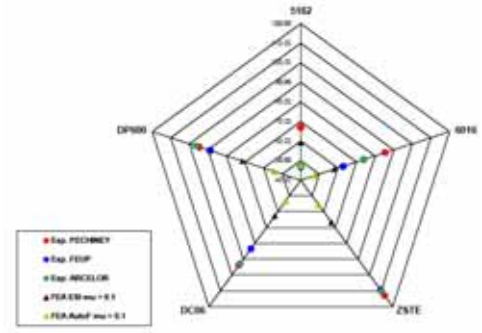

Figure 29. Experimental forces compared to calculated ones – Medium BHF

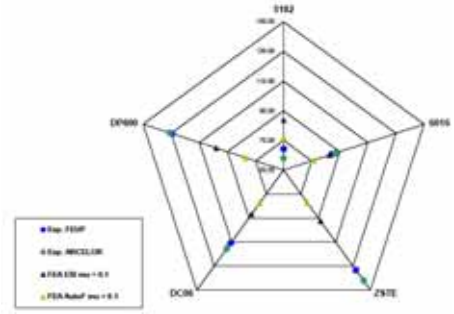

Figure 30. Experimental forces compared to calculated ones – High BHF

For steels, comparison with simulations show that numerical prediction is always distinctly under the experimental value for a friction condition set to 0.1. AUTOFORM delivers the smallest values of force (sometimes at half of the true ones).

It's the same for aluminum alloys but, on the contrary, using the variable coefficient of friction, too high forces are estimated. From this point of view, it seems that the best result could be found with a coefficient of friction situated between 0.10 and the measured variable values (which are around 0.20).

To evaluate the characteristic angles, the NXT Post Processor is used from the rough result measured with the experimental apparatus or calculated by the FEA software. For the sake of simplification we will only present figures giving the comparisons relative to the flange angle α 1 and α 2 for two different materials. In fact, differences originate from the wall curvature.

- AA5182 alloy

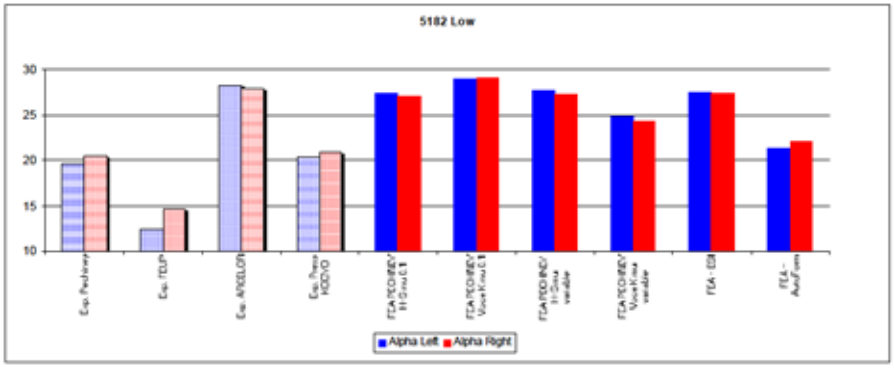

Figure 31. Aluminum alloy 5182 – BHF Low – α evaluation

Concerning the AA5182 alloy, it can be seen that the simulations conform well with Usinor experimental results, the ones showing the more springback. We remind that there was also no increase of punch force during forming, so probably Usinor data are the closest to the definition of the 0.1 coefficient of friction. If compared to the Usinor experiments, PAMSTAMP springback evaluation is good, AUTOFORM slightly too small. It is confirmed that the Hocket-Sherby and Voce laws are well adapted to this alloy.

-DP600 steel

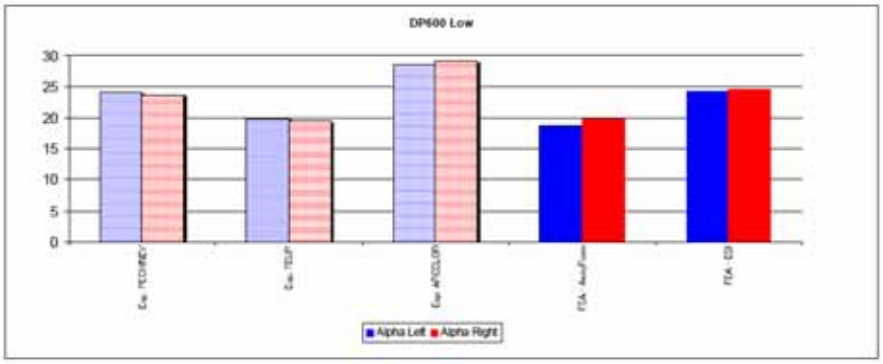

Figure 32. DP600 steel – BHF Low – α evaluation

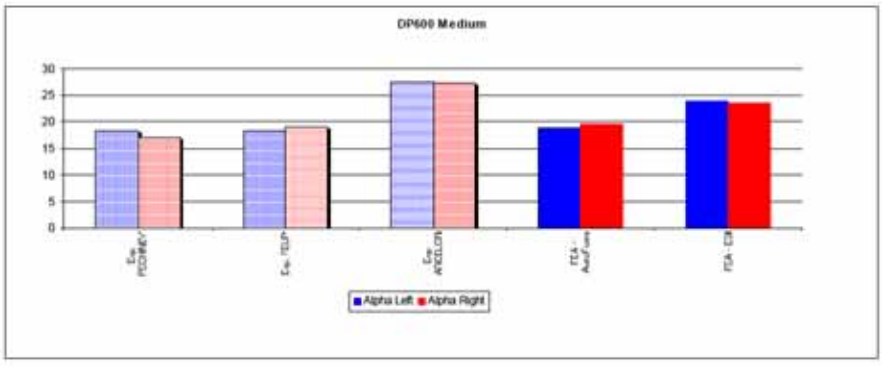

Figure 33. DP600 steel – BHF Medium – α evaluation

AUTOFORM calculated α angles are very close to the ones measured in FEUP and Pechiney experiments. Those given by PAMSTAMP approximately give a mean value for all the partner's experiments. It must be noted that the use of a higher coefficient of friction, as suggested by the forces comparisons, would normally reduce again the calculated angles.

Conclusion for this benchmark #1:

- forces prediction is always too small with a coefficient of friction = 0.1 and too high with a coefficient close to 0.2,
- using the coefficient of 0.1, springback simulations are in good accordance with Usinor experiments for aluminum alloys. This is a good result because the Usinor experiments seem to be the less perturbed by friction problems,
- generally speaking, predictions are not so bad, the calculations by AUTOFORM being always slightly under the ones of PAMSTAMP.

Benchmark #2

A considerable amount of simulation was conducted: 96 with a coefficient of friction of 0.1, plus 23 with a variable coefficient of friction (according to tribological experiments). All five laws indicated before were studied with PAMSTAMP2G and DD3IMP. In AUTOFORM was examined the effect of Swift and Voce laws, and Swift only in LS-DYNA. In order to judge rapidly and easily the validity of comparisons, it was chosen to use the ratio "simulation / experiment" concerning all the angles measured on a rail. In the next table, only values concerning α angle are presented. However, as this angle can be very small, the ratio can reach unrealistic values. To avoid this inconvenient, we do not consider directly α but the angle "90° - α ". Of course, the closer the ratio from 1, the better the result. Table 11 is relative to Low BHF.

Table 11. Ratio of simulation / experiment for the angles 90° - α (friction coeff. = 0.1)

BHF = 90 kN, μ = 0.1							
Material			5182	6016	DC06	DP600	HSLA
PAM2G	Swift	90-Alpha	0.91	0.93	0.96	0.92	-
	Voce	90-Alpha	-	-	-	0.94	-
	Swift-Sat.	90-Alpha	-	-	-	0.97	-
	Voce-Sat.	90-Alpha	-	-	-	0.95	-
	Teodosiu-Hu	90-Alpha	-	-	-	0.97	0.96
AUTOFORM	Swift	90-Alpha	0.97	0.98	0.99	0.99	0.98
	Voce	90-Alpha	-	-	-	0.98	-
DD3IMP	Swift	90-Alpha	0.93	0.94	0.98	0.95	0.96
	Voce	90-Alpha	0.93	0.94	0.98	0.95	0.96
	Swift-Sat.	90-Alpha	0.94	0.94	0.99	0.97	0.97
	Voce-Sat.	90-Alpha	0.93	0.94	0.99	0.97	0.97
	Teodosiu-Hu	90-Alpha	0.96	0.96	0.99	0.98	0.97
LS-DYNA	Swift	90-Alpha	0.96	0.95	-	-	-

Generally speaking, the prediction is never far from the reality. With PAMSTAMP2G, DD3IMP and LS-DYNA, the Swift law is aluminum alloys and for the DP steel. This is not surprising because supposed to closely follow this law. But AUTOFORM seems to work well with this law. This probably influence of the structure of the code on the performance given by the chosen for the material, and not only a physical influence of this one.

In all cases where it was implemented, the Teodosiu-Hu microstructural model gives the better estimation of the springback. The following example concerns the use of a variable coefficient of friction as defined by our experiments in WP3.

Table 12. Ratio of simulation / experiment for the angles 90° - α (variable friction coeff.)

BHF = 200kN, variable μ coefficient							
Material			5182	6016	DC06	DP600	HSLA
AUTOFORM	Swift	90-Alpha	1.03	1.03	1.01	0.95	0.99
	Voce	90-Alpha	-	-	-	-	-
DD3IMP	Swift	90-Alpha	1.00	1.01	1.01	0.92	0.99
	Voce	90-Alpha	-	-	-	-	-
	Swift-Sat.	90-Alpha	-	-	-	-	-
	Voce-Sat.	90-Alpha	-	-	-	-	-
	Teodosiu-Hu	90-Alpha	1.01	1.03	1.02	0.94	1.00
LSDYNA	Swift	90-Alpha	1.02	-	1.01	0.92	0.98

There is a slight tendency to underestimation of the α angle (we measure “90° - α ", so that a ratio over 1 means that α is slightly too small). This is most probably due to the fact that the coefficients of friction used with the “variable coefficients” are higher that the conventional value of 0.1. Anyway, the calculated angle values are very close to the experimental ones. We can again see that the Swift law is definitely not adapted to the DP600 steel.

Benchmark #3

Several partners have performed experiments with benchmark #3. However, profile measurement of such experiments has been only performed by FEUP. This is the reason why FEUP is the only experimental partner to be used in this report for comparison with simulation results. The sections to be measured are shown on figure 34.

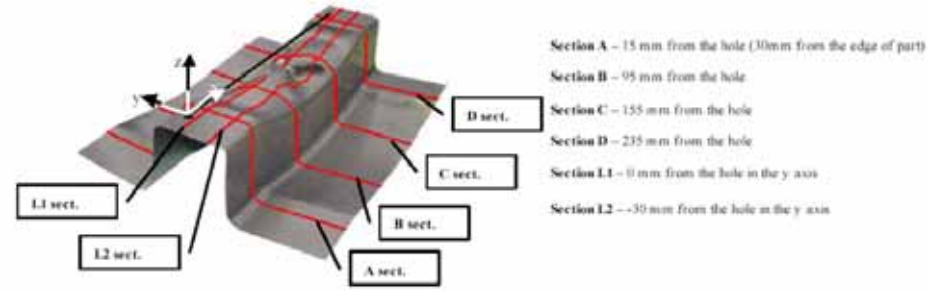

Figure 34. Sections to be measured on part #3

This benchmark gives the opportunity to compare the evolution of force as predicted by several software. Figure 35 (DC06 steel at Low BHF) shows this evolution compared to the experimental one given by FEUP tests. The curve given by OPTRIS is in most cases the highest, followed by the ones of AUTOFORM then PAMSTAMP. Here are two curves relative to this code: one obtained by Press Kogyo, exactly on the experimental curve, and the other obtained by ESI which is lower.The case of AUTOFORM is particular: there is always a maximum at start (about 25 mm) followed by a large decrease.

Color key: red: FEUP experiment

blue : Volvo simulation (AUTOFORM)

dark blue : Volvo simulation (LS-DYNA)

light blue : UTS simulation (OPTRIS)

magenta : ESI (PAMSTAMP2G)

orange : Press Kogyo (PAMSTAMP), curves confused with experiment

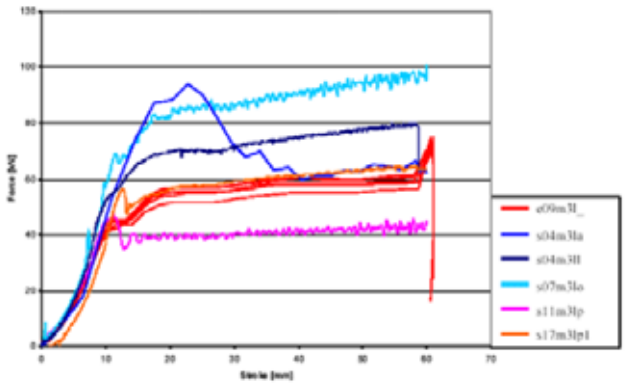

Figure 35. Evolution of punch force – DC06, Low BHF

Some remarks:

- the shape of the AUTOFORM curve is quite probably due to the initial wrinkling of material.

It can be explained in two ways: i) due to its structure, this code is not at all designed to tackle wrinkles, ii) the triangular elements probably introduce some exaggerated stiffness,

- two partners, ESI and Press Kogyo, using the same code with theoretically the same data and conditions obtained results differing by 50 %,
- these observations apply for the case of “normal” punch force evolution, that is excluding the cases where we observed an abnormal increase due to galling.

In conclusion, the prediction of forming effort does not seem to be very reliable today.

However, we must recognize that the case was difficult because of the strong wrinkling at start of forming. Springback prediction is shown by the following table.

Table 13. Angles α 2 measured or calculated for section B

		FEUP	Press K	Volvo	P. K.	Volvo	ESI	P. K.	UTS
		Experi.	Autof.	Autof.	Itas-3D	LS-Dyna	Pam-stamp	Pam-stamp	Optris
AA5182	90	13		7	14	5	18		17
AA6016	90	11	4	7		6	14	10	
DC06	90	7	4	6		7	10	10	8
	200	2		3		7	8		
	300	1		2		5	6		
HSLA	90	10		5			11		12
	200	4		3		7	8		
	300	1		2		5	6		
DP600	90	18	8	8		10	16	15	17
	200	12		5		12	14		
	300	11		4		10	12		

Comments:

- the implicit Japanese code ITAS-3D is excellent for the springback prediction although slow when compared to explicit codes,
- PAMSTAMP and OPTRIS also deliver reasonable values,
- LS-DYNA and AUTOFORM generally underestimate the springback.

Benchmark #4

The punch forces estimations exhibit very great differences as seen on figure 36 for the AA5182, Low BHF and figure 38 for DC06 at Low BHF. On these figures, green and blue curves represent OPTRIS used with the variable coefficient of friction and OPTRIS used with 0.1 appears in red and yellow (confound lines).

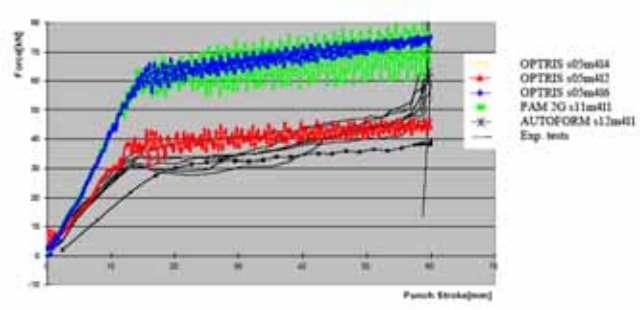

Figure 36. Punch force estimation for the AA5182 alloy with Low BHF

It appears clearly that both simulations using the variable coefficients (about 0.2) indicate punch forces largely over the experimental values. Other results are well in accordance with the latter.

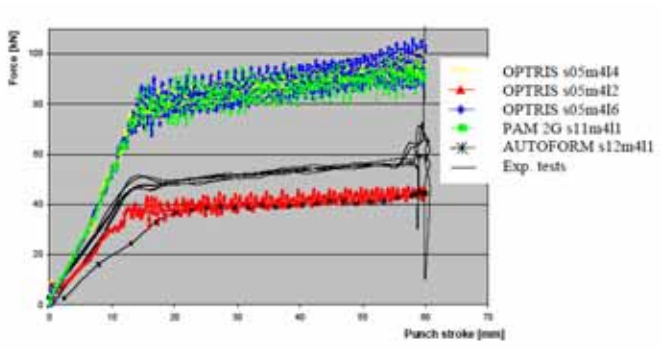

Figure 37. Punch force estimation for the DC06 steel with Low BHF

There are relatively great differences between the profiles calculated with the different codes or options. One example is shown on figure 38 for the AA5182 with Low BHF.

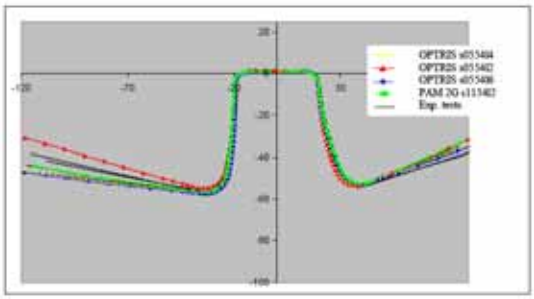

Figure 38. Experimental and calculated profiles for AA5182, Low BHF, section C

In order to make things clear, we have compared the calculated angles $\theta 1$, $\theta 2$.. $\theta 6$ with the experimental values for profiles A and C with the AA5182 alloy.

Table 14. Comparison of angles for AA5182, Low BHF, A profile

		AUTOFORM (0.1- no refin.)	OPTRIS (0.1- 3 lev)	OPTRIS (var- 3 lev)	OPTRIS (var- 4 lev)	PAM 2G (var-1 lev)	Min of exp.	Max of exp.
θ_1	Die radius 1	2.45	0.16	-0.53	0.98	1.89	-0.07	3.99
θ_2	Wall 1	10.61	13.55	10.00	11.18	12.93	8.83	12.69
θ_3	Punch radius 1	2.65	0.52	2.37	2.69	5.56	1.67	5.24
θ_4	Punch radius 2	2.26	0.71	2.88	3.79	6.46	3.76	6.96
θ_5	Wall 2	17.76	21.79	18.49	18.12	17.80	12.99	18.27
θ_6	Die radius 2	2.93	0.11	-0.30	3.65	-0.27	0.25	2.30

Table 15. Comparison of angles for AA5182, Low BHF, C profile

		AUTOFORM (0.1- no refin.)	OPTRIS (0.1- 3 lev)	OPTRIS (var- 3 lev)	OPTRIS (var-4 lev)	PAM 2G (var-1 lev)	Min of exp.	Max of exp.
θ_1	Die radius 1	8.64	-0.87	1.80	2.69	1.22	-0.05	5.12
θ_2	Wall 1	10.18	10.99	7.55	8.83	8.79	9.61	14.70
θ_3	Punch radius 1	0.00	3.31	0.91	1.75	2.17	1.32	3.45
θ_4	Punch radius 2	4.21	1.61	4.09	5.27	6.55	4.14	6.57
θ_5	Wall 2	17.12	19.11	18.60	18.63	18.33	15.53	19.61
θ_6	Die radius 2	4.07	-2.91	1.17	4.27	0.97	0.79	5.33

AUTOFORM is good in prediction except for punch angles.

OPTRIS, in standard modelisation, is not too bad but inferior in prediction quality, although two simulations with OPTRIS show that a more realistic friction and a smaller mesh size improve results. PAMSTAMP, with small mesh and more realistic friction coefficient, is generally good in prediction. Results are improved with more realistic friction coefficient (higher coefficients). The same comparisons are now carried out on the DC06 material.

Table 16. Comparison of angles for DC06, Low BHF, A profile

		AUTOFORM (0.1- no refin.)	OPTRIS (0.1- 3 lev)	OPTRIS (var- 3 lev)	OPTRIS (var- 4 lev)	PAM 2G (var-1 lev)	Min of exp.	Max of exp.
θ_1	Die radius 1	0.95	1.76	0.60	0.58	0.21	-0.99	1.27
θ_2	Wall 1	3.49	5.96	4.04	7.16	5.67	2.05	3.99
θ_3	Punch radius 1	0.78	3.53	3.23	3.87	3.59	1.37	3.63
θ_4	Punch radius 2	3.49	3.32	3.95	2.83	3.75	2.18	3.21
θ_5	Wall 2	7.33	10.04	8.26	5.66	8.46	1.21	7.63
θ_6	Die radius 2	1.03	0.40	0.76	0.92	-0.99	-1.47	1.34

Table 17. Comparison of angles for DC06, Low BHF, C profile

		AUTOFORM (0.1- no refin.)	OPTRIS (0.1- 3 lev)	OPTRIS (var- 3 lev)	OPTRIS (var- 4 lev)	PAM 2G (var-1 lev)	Min of exp.	Max of exp.
θ_1	Die radius 1	2.20	2.26	0.56	0.73	-1.02	-1.16	2.38
θ_2	Wall 1	4.38	6.49	1.05	8.07	2.86	3.22	6.37
θ_3	Punch radius 1	-0.29	1.51	2.12	4.03	1.20	-0.26	2.23
θ_4	Punch radius 2	1.81	4.21	3.96	2.41	3.91	1.92	3.97
θ_5	Wall 2	8.02	8.78	7.14	1.93	8.96	2.20	5.82
θ_6	Die radius 2	1.90	-0.23	-0.45	0.81	-0.76	-1.79	0.48

Again, AUTOFORM is good in prediction except for punch angles.

In standard modelisation, OPTRIS is good in prediction except for walls opening, which is overestimated. Nevertheless, two simulations with OPTRIS show that a more realistic friction and a smaller mesh size have an influence on springback results. With OPTRIS, we have different, but not improved, results with mesh size at 1 mm compared to results at 2.5 mm (results not shown in tables). Standard OPTRIS mesh size is not small enough to have results independent to mesh size.PAMSTAMP, with small mesh and higher friction parameters, does not perform as well as for the AA5182.

From these results, it seems that a uniform friction is not as convenient as a variable one. However, it is impossible, with these tests, to separate the influence of a variable friction coefficient (that is, adapted to each part of the tool) from the fact that the variable coefficients are significantly higher than the conventional 0.1.

Twisting is measured on the upper side of the part by comparing relative body movements of both extremities. Unfortunately, we only have these values for two materials, AA5182 and DC06. In all cases, the twist angle is relatively small, inferior to our expectations. It would have been interesting to see the figures for DP600 and HSLA steels.

Table 18. Comparison of twisting angles for AA 5182 and DC06, Low BHF

Twist angle	AUTOFORM (0.1- no refin.)	OPTRIS (0.1- 3 lev)	OPTRIS (var- 3 lev)	OPTRIS (var.- 4 lev)	PAM 2G (var-1 lev)	Min of exp.	Max of exp.
5182	0.81	-1.21	0.11	0.28	-0.02	0.01	1.11
DC06	-0.61	0.10	-0.78	-0.51	-0.77	-0.43	0.51

AUTOFORM overestimate twisting in one direction.

OPTRIS gives good result in standard configuration and overestimate results with higher friction coefficients. PAMSTAMP2G slightly overestimate twisting as OPTRIS, perhaps because of higher friction coefficients. Increasing the level of refinement slightly increase the tendency to twisting (result not shown in table). But due to the small angles we found, it is not certain that such conclusions are truly representative. ESI used this benchmark for a deep study concerning an option called ”the line search option”. They concluded that it is essential to introduce it in the following version 2004 of Pam Stamp 2G.

Benchmark #5

Concerning experiments, only one tool has been constructed by DaimlerChrysler. This tool was sent to Olofström to be used by Volvo but a diaphragm rupture stopped these trials. Finally, trials were made with the sheet material from Volvo but in the DaimlerChrysler press shop. They are not different from the DaimlerChrysler ones. Simulations have been conducted by DaimlerChrysler with OPTRIS and ESI with PAMSTAMP2G (only for AA5182, low BHF). The larger deviation from theoretical profile is found in section C. We illustrate it by two figures from DaimlerChrysler and ESI studies which are, unfortunately, inverted and not at the same scale.

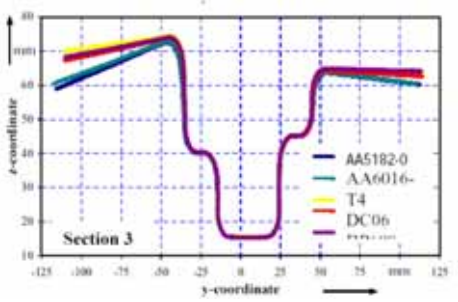

Figure 39. Calculation made by DaimlerChrysler on section C - AA5182 alloy

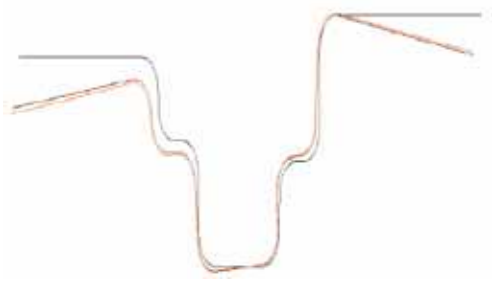

Figure 40. Calculation made by ESI on section C - AA5182 alloy

There is a big similitude of profile, the α angles being respectively:

- hole side : 26° for DCAG and 22° for ESI,
- opposite side: 13° for DCAG and 15° for ESI, a result which is reproduced for other sections.

It is more difficult to evaluate springback because it appears in two ways: the level of the curves depends from the general transverse springback as illustrated in figures 39 or 40 while the variation of shape is due to variation of this springback along the measured line. This is why we do not develop more the results obtained in this benchmark.

Benchmark #6

Four materials only were considered because the AA5185 alloy exhibits Lüders bands and cannot be used for external automotive parts as this panel.

In order to have the same conditions for all codes, a base set-up of parameters was decided in the project. It was also decided that all partners would use the same tool model. Furthermore, two friction set-ups were to be tested. Both constant friction with μ=0.1 and variable friction coefficient which were measured.

The results that were analyzed are:

- Punch forces,
- Draw-in,
- Section profiles,
- Surface defects.

Distribution of strains and stresses is highly inhomogeneous on this panel, as illustrated by figure 41. This due to the fact that the metal situated on the punch summit is not deformed although metal of corners and the embossment are drawn or stretched.

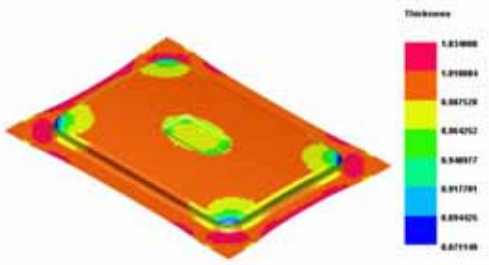

Figure 41. Thickness distribution through the part

Punch forces are compared for two level of stroke: 20 and 35 mm.

Table 19. Punch forces from simulation

Material	Software	Model - friction	Force at 20mm (kN)	Force at 35mm (kN)
AA6016	AutoForm	Swift - 0.1	83	223
	AutoForm	Swift - var.	126	320
	LS-DYNA	Swift - 0.1	103	242
	LS-DYNA	Swift - var.	123	342
	OPTRIS	Kin. - var.	143	325
	PAMSTAMP	Swift - 0.1	103	243
		Exp. Average	*127*	*289*
DC06	AutoForm	Swift - 0.1	79	230
	AutoForm	Swift - var.	136	385
	LS-DYNA	Swift - 0.1	90	240
	LS-DYNA	Swift - var.	143	400
	OPTRIS	Kin. - var.	127	311
	OPTRIS	Swift - 0.1	89	220
	PAMSTAMP	Swift - 0.1	89	221
		Exp. Average	*114*	*300*
HSLA	AutoForm	Swift - 0.1	96	225
	AutoForm	Swift - var.	159	390
	LS-DYNA	Swift - 0.1	119	248
	LS-DYNA	Swift - var.	157	349
	PAMSTAMP	Swift - 0.1	123	276
		Exp. Average	*148*	*341*
DP600	AutoForm	Swift - 0.1	117	292
	AutoForm	Swift - var.	187	488
	LS-DYNA	Swift - 0.1	137	317
	LS-DYNA	Swift - var.	179	438
	PAMSTAMP	Swift - 0.1	135	300
		Exp. Average	*149*	*342*

For all materials was the same tendency achieved. Where μ=0.1 was used the forces were underestimated and when the measured friction was used the forces were overestimated. The prediction was rather poor for both cases. If we now look at draw-in, a comparison of estimations to the average experimental results also shows that high friction gives the best correspondence. They are shown in figures 42 and 43.

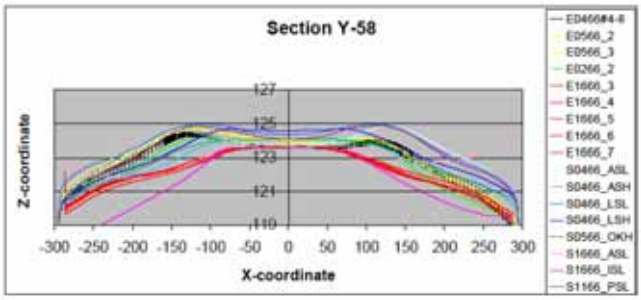

Figure 42. Simulation results for AA6016

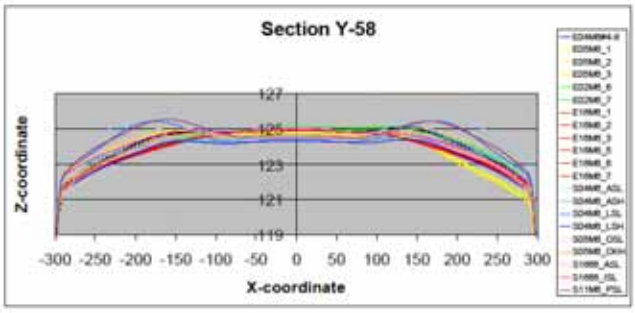

Figure 43. Simulation results for DC06

The qualitative correspondence to experimental results is good, but the simulation exaggerates the results a little.

It is better to analyze results material by material.

AA6016

- Measured friction: the results do not catch the ridge in the middle of the panel,
- μ=0.1: Follow the experimental results better.

All codes have the above-mentioned tendency, except ITAS3D which does not follow the shape of the profile so well.

DC06

- Measured friction: the results correspond to the experimental ones rather well.
- μ=0.1: The results exaggerate the ridge in the middle of the panel.

These results apply for LSDYNA, AutoForm and PAMSTAMP (only μ=0.1). ITAS3D results correspond well to the experimental results. The hardening law was tested in OPTRIS and gave that kinematic hardening and μ=0.15 gives a better result as compared to isotropic hardening and μ=0.1.

HSLA

- Measured friction: LSDYNA - The results corresponds to the experimental results but the ridges are exaggerated.

  AF - The results correspond to the experimental results rather well.
- μ=0.1: LSDYNA - The results exaggerate the ridge in the middle of the panel, but are otherwise rather good.

  AF - The results correspond to the experimental ones rather well, but do not catch the ridge in the middle of the panel.

  PAMSTAMP - The results exaggerate the ridge in the middle of the panel, but are otherwise rather good.

  ITAS3D predicts a wrong shape

The twisting which was indicated in the experimental results was not shown in any of the codes. This is normal: particular precautions must be taken for.

DP600

- Measured friction: LSDYNA – The results correspond well to the experimental results but the ridges are exaggerated (less than for μ=0.1)

  AF - The results underestimate the section and do not catch the ridge in the middle of the panel.
- μ=0.1: LSDYNA - The results exaggerate the ridge in the middle, but are otherwise rather good.

  AF - The results correspond to the experimental results rather well, but exaggerate the ridge in the middle of the panel.

  PAMSTAMP - The results exaggerate the ridge in the middle of the panel, but are otherwise rather good.

Notice: AF-results reported from Nissan and from Volvo differ. The variation could be caused by the use of different settings.

Efficiency of physical models

Pechiney has compared “Hocket-Sherby isotropic” and “Voce + kinematic hardening” for tests with aluminum alloys, low BHF, on tool #1, using OPTRIS. We look at the effect on the flange angle α.

Table 20. Comparison of α angles (mean values) in function of coefficient of friction

	Coefficient = 0.1		Variable coefficient		Usinor
	Hocket-Sherby	Voce + K	Hocket-Sherby	Voce + K	Experiment
AA 5182	27	29	27	24.5	27.5
AA 6016	22.5 *	25.5 *	26	25.5	27

* large variation between right and left sides

There is not a big influence of the chosen model upon the α angle. It must be noted that results are the same for θ 3 angles (wall curl).

For tool #2, we present the results obtained for the DP600 steel, low BHF, using the codes PAMSTAMP2G and AUTOFORM.

With PAMSTAMP2G, introducing some saturation has a beneficial effect for this steel. The microstructural Teodosiu-Hu model conducts to the best results with this code. AUTOFORM obtains even better results with classical Swift and Voce laws.

Next table shows the same type of results obtained with the code DD3IMP, where all of the project proposed models were implemented and tested.

Table 21. Ratio of sim. / exp. for the angles 90° - α (friction coeff. = 0.1, low BHF)

	DD3IMP				
	Swift	Voce	Swift-Sat.	Voce-Sat.	Teodosiu-Hu
AA5182	0.93	0.93	0.94	0.93	0.96
AA6016	0.94	0.94	0.94	0.94	0.96
DC06	0.98	0.98	0.99	0.99	0.99
HSLA	0.95	0.95	0.97	0.97	0.98
DP600	0.96	0.96	0.96	0.97	0.97

For all materials, the best result is with the Teodosiu-Hu microstructural model. For other models, there seems to be a slight advantage to using saturation with the exception of AA6016. The results for medium BHF are presented next. First, we present them for the 0.1 coefficient of friction.

Table 22. Ratio of sim. / exp. for the angles 90° - α (friction coeff. = 0.1, medium BHF)

	DD3IMP		AUTOFORM	
	Swift	Teodosiu-Hu	Swift	Voce.
AA5182	0.95	0.97		
AA6016	0.95	0.96		
DC06			0.99	0.98
HSLA			0.98	0.97
DP600	0.95	0.98	0.98	0.96

With the code DD3IMP, the Teodosiu-Hu gives slightly better figures, both Swift and Voce laws seem to work well with the AUTOFORM software. Calculations were also performed for the medium BHF, this time with the variable coefficients of friction.

Table 23. Ratio of sim. / exp. for the angles 90°-variable coefficient, medium BHF

	DD3IMP	
	Swift	Teodosiu-Hu
AA5182	1.00	1.01
AA6016	1.01	1.03
DC06	1.01	1.01
HSLA	0.92	0.94
DP600	0.99	1.00

As already noticed, the calculated α angles are smaller (μ is higher). There is a tendency for the Teodosiu-Hu model to give better results for steels, but not for aluminum alloys.

As a general conclusion for this study:

- the microstructural model globally ensures the best results in term of prediction of the total springback (α angle).
- for all materials, the use of a model that includes kinematic hardening in its formulation improves the results accuracy.
- the AUTOFORM software has a peculiar behavior and delivers good results for all materials. The results are apparently independent of the models tested (Swift and Voce law).

Friction models

We used only two models, both based upon the Coulomb's law stating that there is a constant ratio μ between the force F_N applied normal to the material and the resistance F_{frict} resulting from friction:

$$F_{frict} = \quad . F_N$$

The first model we used is a classical one: the coefficient of friction μ was chosen equal to 0.1 for all contact positions between the blank and the tool.

In the second case, variable values were affected to different areas of contact: between blank and binder (die and blank holder), between blank and die radius and also between blank and punch. These values were thoroughly measured by experiments made in WP3. It is worth noting that the actual blank materials, tool materials and lubricant (as well as lubricant amount) used in the project were tested during these experiments. Moreover, three different laboratories well trained with this kind of work (Cockerill, Pechiney and Usinor) measured very well correlated values of friction.

In general, we found relatively high coefficient of friction (around 0.2). No influence of friction was studied for rail #2, 3 and 5.

For tool #1, four simulations with OPTRIS, made by Pechiney, are available: two materials (AA 5182 and AA6016 at low BHF), both with "Voce isotropic" and "Hocket-Sherby kinematic" models and with constant (0.1) and variable coefficients. The result is shown by table 24.

Table 24. Comparison of stamping forces calculated and measured at 20 mm stroke

	Hocket-Sherby		Voce		Experiment
	μ = 0.1	μ variable	μ = 0.1	μ variable	
AA5182	30	56	30	57	28-36
AA6016	30	56	31	57	40-42

While the coefficient of 0.1 is convenient for AA5182, the variable coefficients of friction clearly drove to an overestimation of the stamping force (up to 100 %) for both materials.
With OPTRIS, Renault performed some study of friction influence on tool #4.

Table 25. Comparison of forces calculated and measured at 20 mm stroke, low BHF

	μ = 0.1	μ variable	Experiment
AA5182	39	64	29-38
DC06	40	80	37-50

Clearly, the variable μ gives an overestimation of the stamping force, sometimes two times higher than the real one.
For the studied cases with this tool, there is strictly no influence of the coefficient of friction upon springback (the maximum difference is of the order of one degree).
For tool #6, the draw-in was measured according to figure 44. The larger is the L1, L2 or L3 measure, the smaller was the draw-in of the metal.

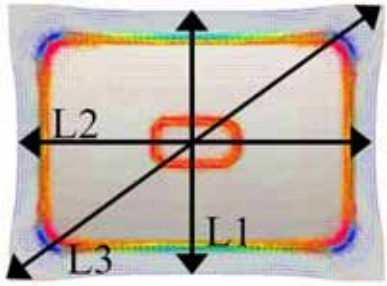

Figure 44. Measurements made to appreciate the draw-in

The results are shown on the next table.

Table 26. Comparison of draw-in on panel

Material	Notation	L1	L2	L3
AA6016	S0466_ASL	515,7	704,9	915,1
	S0466_ASH	518,4	709,4	905,2
	S0466_LSL	516,8	709,2	915,4
	S0466_LSH	518,8	711,7	919,2
	Exp. Average	*518,4*	*711,6*	*924*
DC06	S04M6_ASL	505,4	698	909,5
	S04M6_ASH	515,7	704,9	915,1
	S04M6_LSL	504.8	704.1	911.7
	S04M6_LSH	510.8	704,1	914,7
	Exp. Average	*513,5*	*706,0*	*923*
HSLA	S04H6_ASL	502,5	692	907,8
	S04H6_ASH	506,7	694	915,4
	S04H6_LSL	500,8	695,3	912,3
	S04H6_LSH	503,2	696,2	915,3
	Exp. Average	502,2	694,9	917,5
DP600	S04H6_ASL	504,7	692,0	908,4
	S04h6_ASH	506,2	695	913,5
	S04H6_LSL	500	696,6	908,9
	S04H6_LSH	501,6	697,2	910,8
	Exp. Average	*502,9*	*694,8*	*916,8*

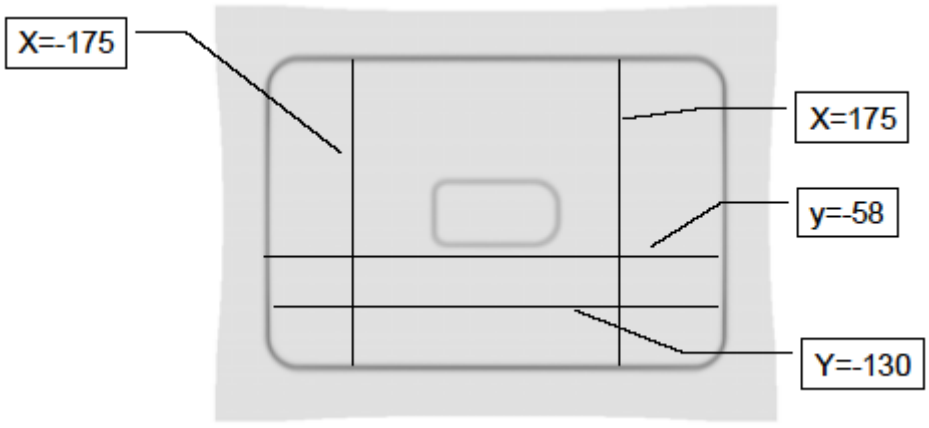

Figure 45. Position of section

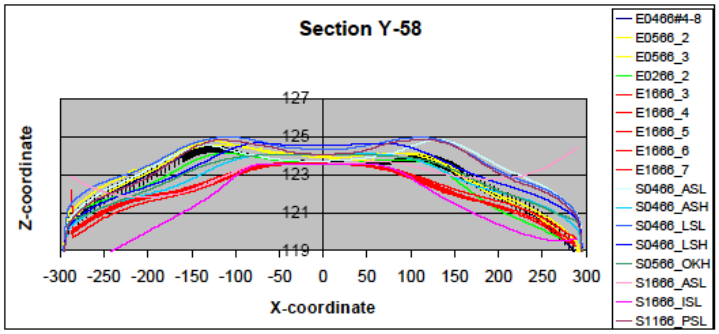

Figure 46. Section of the panel (AA6016)

Although there is some scatter in the experiments, it is considered that the correct profile consists in two ridges (narrow hills) surrounding a central depression. These ridges are a particular form of the so-called “teddy bear ears”.

LS-DYNA:

AA6016. The 0.1 coefficient of friction gives a profile close to reality while variable coefficient does not catch the ridges.

DC06. The 0.1 coefficient exaggerates the ridges while variable is OK.

HSLA. The ridges are exaggerated in both cases.

DP600. The ridges are also exaggerated, but at a less extent with $\mu = 0.1$.

In conclusion for LS-DYNA, the global reduction of the coefficient of friction (the 0.1 case) increases the height of the ridges. This is a logical tendency.

AUTOFORM:

AA6016. The 0.1 coefficient of friction gives a profile close to reality, while the variable coefficient does not catch the ridges (as for LS-DYNA).

DC06. The 0.1 coefficient exaggerates the ridges, while the variable one is OK (as for LSDYNA).

HSLA. The 0.1 coefficient does not catch the ridges while it is done with variable coefficient. This is strange since the variable coefficient is globally higher than the variable one.

DP600. The results with variable μ underestimate the section and do not catch the ridge in the middle of the panel while 0.1 exaggerate the ridges.

Conclusion for AUTOFORM: apart for the case of HSLA, the tendency is also conform to the reality.

Conclusions concerning models

In sheet metal forming, due to the complex materials usually involved, constitutive models based only on isotropic work-hardening (like Swift or Voce models) are often not accurate enough. Of course, the efficiency of a model cannot be judged globally: it depends of the

characteristics of the software in which it is implemented. The project shows that the microstructural Teodosiu-Hu model gives the best results concerning springback. Also, it was observed for all materials that the models including kinematic hardening conduct to better results than models based only on isotropic work hardening. These last models (Swift and Voce) don't show significant different results (for example, the tests with AUTOFORM give the same results, whether Swift or Voce laws are used). This is clearly associated with the low level of strain attained in the drawn parts, making the prediction of these two models very similar. Meanwhile, it is clear from the present results that the differences between the various tested models are never very large. For the rails, this could be partly attributed to the small amount of strain after drawn and to the relatively large die radius chosen for these experiments: 10 mm are convenient for the aluminum alloys but not for steels. Some authors have noticed that the favorable influence of the kinematic hardening models is only visible in case of strong bending-unbending.

For accuracy purposes the last conclusions could be stated in a different way: even for so large die radius and so small strains after drawn the use of more accurate constitutive models shows clear advantages in terms of accuracy of results. There are some concerns with the influence of friction. Using the classical value of 0.1 for the coefficient of friction leads to underestimation of forces. Using the experimental values measured in our tribological experiments leads to overestimated punch forces. However, predicted springback is not so much sensitive to friction, while it is very much in experiments. This undoubtedly raises some interrogation. Is the friction well represented in simulation? First, it must be said that the friction behavior is probably, for the time being, one of the less known and understood phenomena of sheet metal forming. It is probably not exaggerated to say that the mechanical behavior of the material itself, through strain hardening laws and plasticity criteria, has received very much more attention than friction. There could be two important causes of our lack of knowledge:

- one is experimental: we are not able to know or measure precisely the coefficient of friction in a given area of a tool. We are no more able to define a precise influence of the sliding speed on this coefficient and its variation during a stroke. This was clearly revealed by this project. We have a need for evaluative friction law, but it represents a considerable amount of experiment.
- the other is numerical: it is very difficult to obtain a good representation of the contact of two surfaces when they consist of small elements. Opinions differ about it: some think that it will never be possible. Some others are more optimistic.

In any case, friction is certainly an area where many studies are still needed if we want to progress in understanding and simulation of sheet metal forming.

4. Project Administration

4.1 Project Management Structure

The project management was organized so as to ensure an extensive international collaboration with minimal administrative cost and efficient use of time and resources. The Inter-regional management structure of the 3DS project is shown in Figure 47. It consisted of a steering committee, a technical committee, and working package leaders. The Steering Committee had the overall responsibility of the project. It comprised the Regional Co-ordinating Partners and Inter-regional Co-ordinating Partner. The technical management is carried out by the Technical Committee, who set the research directions according to the objectives, and by the Work Package Leaders, who gave advice on the research. Resolutions by the Technical Committee were made by unanimity.

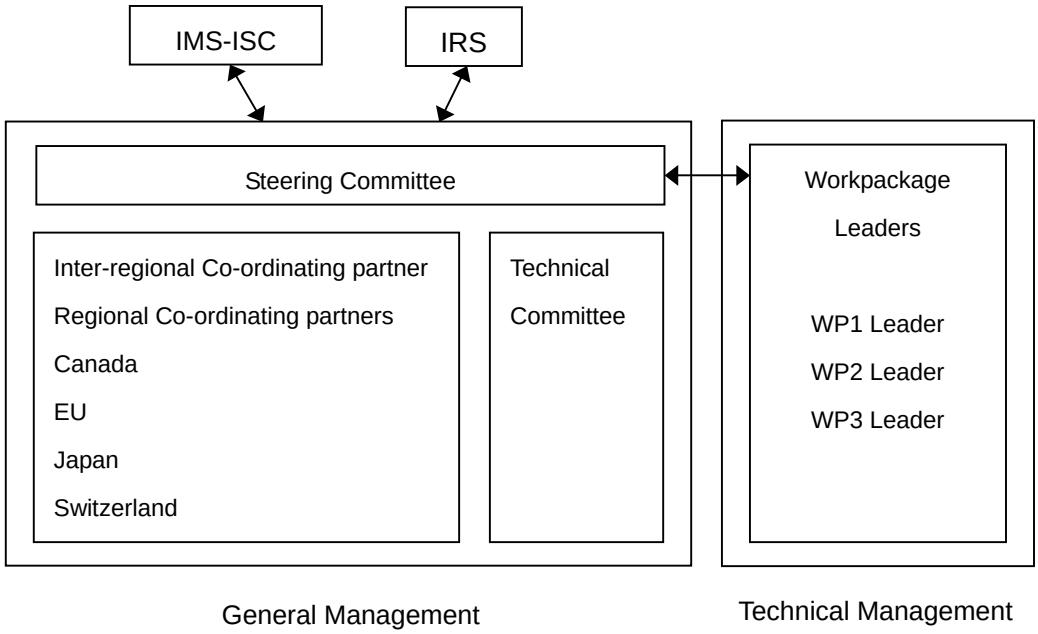

Figure 47. The 3DS Management Structure

4.2 Administrative Structure

The 3DS Steering Committee met at least twice a year and the Consortium partners attended at least one of these meetings. The Technical Committee met several times a year as necessary. Both the Steering Committee and Technical Committee reviewed at their respective meetings reports from the work packages to ensure that the works were in progress according to the plans, producing results as expected.

The Workpackage Leaders organized " video conferences" at an interval of one or one and

half month to maintain continuous contact with the partners in the workpackages in their respective care. The videoconferences proved very helpful to avoid misunderstandings among the partners in a given workpackage about its goals, and delays in schedule, which may have arisen without them.

A general meeting of all consortium partners was held at every milestone of the project.

4.3 Communication Infrastructure

During the preparatory stage of this project, we used electronic mail to exchange information among partners. It was fast and worked very well. However, once the project started, information to be exchanged, including data from experimental work and those for presentation grew too large in size for us to handle by e-mail.

In order to solve this problem, we set up a common server called “Project Extranet Server” that permits partners to share and manage information. This server consisted of features such as a “Cabinet” for uploading and downloading experimental data, meeting minutes etc., a “Bulletin Board” for communication among partners, a “Scheduler” for notification of schedule, a “Circulation” for circulating information among partners, and a “Forum“ for discussion among partners. This server allowed the partners to obtain necessary information, how large data size was, from any region at any time. It is not an exaggeration to say that this server facilitated global communication, that is one of important issues in the international collaboration. The server provided an excellent and efficient environment for the collaboration.

5. Consortium Composition

3DS project was conducted by an international consortium details of which are given below:

5.1 Regions involved and ICP/RCP

Regions Involved: Japan, EU, Canada, and Switzerland

International Coordinating Partner (ICP): CIMTOPS CORPORATION

Regional Coordinating Partners (RCP):
Japanese Region: CIMTOPS CORPORATION
European Union Region: ARCELOR
Canadian Region: Forming Technologies Incorporated
Swiss Region: AutoForm Engineering GmbH

5.2 Consortium Partners

[Canada Region]

Industrial Partners:

Forming Technologies Incorporated

[European Union Region]

Industrial Partners:

ARCELOR (France)
Cockerill-Sambre R&D (Belgium)
ESI (France)
DaimlerChrysler AG (Germany)
Pechiney CRV (France)
Renault (France)
Volvo Car Corporation (Sweden)
UTS S.p.A (Italy)

Academic Partners:

CNRS-LPMTM (France)
FEUP-DEMEGI (Portugal)
DEM-FCTUC (Portugal)

[Japan Region]

Industrial Partners:

CIMTOPS CORPORATION
NISSAN MOTOR Co., Ltd.
PRESS KOGYO Co., Ltd.
TSUBAMEX Co., Ltd.

Academic Partners:

Osaka Institute of Technology, Dept. of Mechanical Engng.
The University of Tokyo, Institute of Industrial Science
GSIS of Tohoku University
Tokyo University of Agriculture and Technology
FUKUSHIMA National College of Technology

[Switzerland Region]

Industrial Partners:

AutoForm Engineering GmbH

6. Dissemination of results

In accordance with IMS IPR Provisions and Consortium Collaboration Agreement (CCA), the results of 3DS disseminated through presentation at various conferences, seminars and workshops, as well as publications in scientific journals.